

Molecular structures of supported metal oxide catalysts under different environments

M. A. Bañares^{1*} and I. E. Wachs²

¹ Instituto de Catalisis y Petroleoquímica, CSIC, Campus UAM-Cantoblanco, E-28049 Madrid, Spain

² Zettlemoyer Center for Surface Studies and Department of Chemical Engineering, Lehigh University, Bethlehem, Pennsylvania 18015, USA

Received 3 August 2001; Accepted 15 February 2002

The use of *in situ* Raman spectroscopy to study the molecular structures of supported metal oxide catalysts under different environments is reviewed. The molecular structures under ambient (hydrated) and dehydrated conditions are presented. The effect of moisture at elevated temperatures is also presented and discussed with regard to its implications for catalytic phenomena. The molecular structural transformations during C₂–C₄ lower alkane (LPG) oxidation, methane oxidation, methanol oxidation and selective catalytic reduction of NO with NH₃ reaction conditions are presented. *In situ* spectroscopy during catalytic reaction with simultaneous activity/selectivity measurement ('operando' spectroscopy) is emphasized owing to its contribution to the fundamental understanding of catalytic performance. The reducibility of the different surface metal oxide species, the relevance of surface coverage (surface monomeric vs polymeric species) and the specific oxide support are discussed when LPG, methane, methanol or hydrogen is the reducing agent. *In situ* Raman spectroscopy provides molecular-level information about the surface metal oxide species: structures, stability and transformations under different environments. In many cases, the use of complementary spectroscopic techniques results in a more complete understanding of the molecular structure–activity/selectivity relationships for supported metal oxide catalysts. Copyright © 2002 John Wiley & Sons, Ltd.

INTRODUCTION

Raman spectroscopy is an extremely powerful catalyst characterization technique because it can provide fundamental information about catalytic molecular structures and surface reaction intermediates. Furthermore, Raman spectroscopy can provide this information under *in situ* conditions (temperature, partial pressure of gas phase components, etc.).¹ Consequently, Raman spectroscopy has been used to examine essentially all types of catalytic materials: bulk and supported metals, bulk mixed metal oxides, supported metal oxides, bulk and supported metal sulfides, zeolites and molecular sieves, heteropolyoxo anions and clays.² The combination of fundamental molecular structural information and *in situ* capabilities has resulted in a powerful tool for catalysis science, which allows for the development of a molecular-level understanding of structure–activity/selectivity relationships for catalytic reactions.

Several publications have extensively reviewed the contributions of Raman studies in catalysis.^{3–17} This paper, however, must only review the Raman studies of catalysts performed over the past decade at Lehigh University (USA) and the Institute of Catalysis and Petroleum Chemistry (Spain). In particular, the use of Raman spectroscopy to study supported metal oxides under the following environments is presented: ambient conditions (hydrated), dehydrated conditions, wet oxidation reaction conditions, oxidation reaction conditions (alkane oxidation, methanol oxidation and selective catalytic reduction of NO_x) and under reducing conditions (by alkanes or by hydrogen, with subsequent reoxidation). The role of the environment (dry air, humid air, reaction conditions, etc.) on the structural transformations of supported metal oxides is also discussed. The combination of fundamental molecular structural information and *in situ* capabilities has resulted in an explosion of Raman spectroscopic characterization studies in the catalysis literature that began in the 1970s, from three publications in 1970 to ~140 publications in 1999.^{2,9} Among those published in 1999, about 30 correspond to Raman studies of supported metal oxides.² In recent years, there has been an emphasis on the molecular characterization of catalysts under reaction conditions since such fundamental information should lead to the development of molecular structure–activity/selectivity relationships and

*Correspondence to: M. A. Bañares, Instituto de Catalisis y Petroleoquímica, CSIC, Campus UAM-Cantoblanco, E-28049 Madrid, Spain. E-mail: mbanares@icp.csic.es

Contract/grant sponsor: National Science Foundation;

Contract/grant number: CTS-9901643.

Contract/grant sponsor: US Department of Energy, Basic Energy Sciences; Contract/grant number: DE-FG02-93ER14350.

Contract/grant sponsor: CICYT; Contract/grant numbers: QUI98-0784; IN96-0053.

the molecular engineering of improved catalytic materials. At present, this is resulting in spectroscopic studies of catalysts under real reaction conditions, where structure and activity/selectivity are measured simultaneously. This 'real' reaction *in situ* spectroscopy is given the tentative name 'operando,' by one of the authors (M.A.B.), to provide a simple word which underlines the simultaneous evaluation of both structure and activity/selectivity. This name has been borrowed from the Latin gerund 'operando,' which means working or operating, since the spectra are of an 'operating' catalyst. Operando spectroscopy is poised to become a powerful tool in catalysis research.¹⁶ These developments may also be of use in other fields where environmental (temperature, pressure and atmosphere) spectroscopy will provide fundamental information about the molecular structure and performance of various materials.²

Supported metal oxide catalysts generally consist of two-dimensional surface metal oxide overlayers on an oxide support (e.g. alumina, titania, zirconia, silica). The oxide support are typically of ca 10–300 m² g⁻¹. In addition to the two-dimensional surface metal oxide overlayer, small metal oxide crystallites may also be present. The metal oxide crystallites tend to form when (a) the precursor salt is poorly distributed over the support in the catalyst synthesis step, (b) there is a weak interaction between the deposited metal oxide and the underlying oxide support (e.g. metal oxides on silica) or (c) monolayer coverage has been exceeded.

Detailed fundamental surface information on a molecular level can be obtained from model supported metal oxide catalysts containing the two-dimensional overlayers of surface metal oxides.^{4,7,11} A unique feature of supported metal oxide catalysts is that the active component is exclusively present as a surface phase, 100% dispersion, below monolayer coverage and there is no spectroscopic complication from the co-existence of bulk crystalline phases. The only bulk crystalline phase present below monolayer coverage is due to the oxide supports, which tend to give rise to weak Raman signals (e.g. Al₂O₃, SiO₂) or Raman signals that generally occur at much lower wavenumbers than the active supported metal oxide species (e.g. CeO₂, ZrO₂, TiO₂).

Supported metal oxide catalysts are widely employed in industrial applications: alkane dehydrogenation, olefin polymerization, olefin metathesis, selective oxidation/ammoxidation/reduction of organic molecules and inorganic emissions as well as precursors to supported HDS and metallic hydrotreating catalysts.^{7,11,18–20} The use of supported metal oxide catalysts for oxidation reactions has grown significantly over the past few decades owing to their excellent catalytic properties in the manufacture of many chemical intermediates and pollution control strategies.²¹

Supported metal oxide catalysts are ideally suited for Raman spectroscopic studies because the dispersed metal oxide phases generally give rise to strong Raman signals and the oxide support tends to possess weak Raman signals or strong Raman signals that occur at much lower

wavenumbers. Consequently, Raman spectroscopy provides fundamental information about the surface metal oxides species present in supported metal oxide catalysts: specific location, surface coverage, molecular structure and its potential transformation in different environments, the participation of specific metal oxygen bonds in catalytic oxidation reactions (e.g. with the aid of isotopic tracer studies) and surface acidity/basicity. Raman spectroscopy also provides direct fundamental surface information about the ratio of isolated and polymerized surface metal oxide species, terminal M=O and bridging M—O—M bonds, extent of reduction of the surface oxide species during reaction conditions, influence of the oxide support ligands, influence of acidic/basic metal oxide additives (promoters/poisons) and participation of specific M—O bonds in catalysis (e.g. with the aid of oxygen-18-labeled isotope experiments). The bridging M—O—support bonds possess enough of a covalent character that should result in weak Raman bands.⁷ The intensity of the bridging M—O—support band depends on the covalency of that bond and is, therefore, directly related to the electronegativity of the cations involved. For example, the intensity of the bridging V—O—support bond in supported vanadium oxide catalysts should depend on the electronegativity of the cation of the oxide support (Si⁴⁺ > Al³⁺ > Ti⁴⁺ > Zr⁴⁺). Thus, in the series V₂O₅/SiO₂, V₂O₅/Al₂O₃, V₂O₅/TiO₂, V₂O₅/ZrO₂, the polarizability of the bridging V—O—support bond increases, and the Raman signal of the bridging V—O—support bond increases. Thus, bridging V—O—support bonds have not been observed for V₂O₅/SiO₂, V₂O₅ or Al₂O₃ owing to the higher electronegativity of Si and Al cations in silica²² and alumina,²³ so they must be very weak or possibly inactive in Raman. For V₂O₅/TiO₂, the bridging V—O—Ti bond should exhibit weak Raman bands near 638 and 248 cm⁻¹ that cannot be detected owing to the very intense Raman bands of the titania support. However, they are visible on a system where vanadium oxide is supported on a substrate where titania is highly dispersed as a surface species on silica.²⁴ Similarly, the bridging V—O—Zr bond also exhibits weak Raman bands that are visible when vanadium oxide is supported on a system where zirconia is highly dispersed on silica.²⁵ Raman spectroscopy also provides structural information about the presence of microcrystallites (<40 Å), XRD amorphous particles and surface reaction intermediates.

The results presented in this paper are from investigations performed at Lehigh University and Instituto de Catalisis y Petroleoquimica, CSIC. The Raman system used at Lehigh University is a triple-grating spectrometer (Spex, Model 1877), a CCD detector and an argon ion laser. The *in situ* Raman studies were run in a quartz cell with a sample holder made of metal alloy (Hastalloy C), and a 100–200 mg sample disc is held by the cap of the sample holder. The sample holder is mounted on a ceramic shaft that is rotated by a 115 V CD motor at a speed of 1000–2000 rpm. A cylindrical heating coil surrounding the quartz cell is used to heat the

cell. The quartz cell is capable of operating up to 873 K and flowing gas is introduced into the cell at a rate of 50–100 ml min⁻¹ at atmospheric pressure. An on-line mass spectrometer is used to monitor the conversion and selectivity of the specific reaction–catalyst system. The Raman system used at the CSIC institute is a Renishaw Micro-Raman System 1000 equipped with a cooled CCD detector (200 K), a holographic super-Notch filter and a 1800 grooves mm⁻¹ grating. The powdered samples were excited with an argon ion laser. *In situ* Raman spectra were run in a Linkam TS-1500 hot stage that allows heating of the powdered sample to 1773 K under a controlled atmosphere or stream of gases. Operando Raman–GC spectra were run with a laboratory-made reaction cell that consists of a fixed-bed quartz microreactor contained by quartz-wool plugs on both ends; the catalyst (ca 170 mg) is in powder form. The reaction feed is controlled by mass flow controllers and the reactor outlet is connected on-line with a gas chromatograph (HP 5890 Series II). The micro-reactor walls have optical quality and no appreciable differences can be observed between the Raman reaction cell and a fixed-bed microreactor. The laser power on the sample was kept below 5 mW to prevent local heating. Specific details of the experimental procedures in the work discussed below can be found in the original papers cited.

AMBIENT CONDITIONS (HYDRATED)

Under ambient conditions, moisture adsorbs on the surface of supported metal oxide catalytic systems and there is extensive solvation of the surface metal oxides (equivalent to ~20–40 monolayers of water). Therefore, the surface chemistry of supported oxides (V, Nb, Ta, Cr, Mo, W and Re) corresponds to that of aqueous solutions. As in aqueous solution, the molecular structure of the metal oxide depends on the concentration and pH of the aqueous system. Many publications have shown that Raman spectroscopy can follow the hydrated molecular structures of these supported metal oxides as a function of oxide loading and the nature of the oxide support.^{20,21,26–29} For instance, in

the case of hydrated supported vanadium oxide catalysts, Raman spectroscopy can efficiently discriminate between the different kind of vanadium oxides present as a function of the specific oxide support and vanadia loading. It was found that the molecular structures of supported transition metal oxide overlayers on different oxide supports (MgO, Al₂O₃, ZrO₂, TiO₂ and SiO₂) are determined by the net pH at the point of zero charge (PZC). Gil-Llambias *et al.*³⁰ have shown that for the V₂O₅/TiO₂ and V₂O₅/Al₂O₃ systems, the pH at PZC of the samples decreases with increasing vanadium oxide loadings (with surface vanadium oxide coverage). The pH at PZC of the supported vanadium oxide catalytic systems is expected to be much lower than the pH at PZC of the oxide support at high surface vanadium oxide coverage and close to that of the oxide support at low surface coverage because the pH at PZC of V₂O₅ is ~0.5. The surface vanadium oxide species depends on the net pH at PZC of the surface and can be predicted from the known vanadium oxide aqueous phase diagram as shown in Table 1 for low and high surface vanadium oxide loadings. At low surface vanadium oxide coverage, the net pH at PZC should closely reflect the specific oxide support. At high surface vanadium oxide coverage, the pH at PZC is significantly lowered owing to the presence of the acidic vanadium oxide overlayer. The qualitative agreement between the predicted hydrated surface vanadium oxide species and the observed hydrated surface vanadium oxide species on the different oxide supports are shown in Table 1 and underlines the influence of the net pH at PZC of each oxide support upon the surface structure of the hydrated surface vanadium species.

For the silica-supported vanadium oxide system, UV–Vis³¹ and EXAFS/XANES³² studies indicate the presence of VO₅ and octahedral coordinated surface vanadium oxide under ambient conditions. The partial hydration of the dehydrated sample changes the color from white to light yellow and the sample becomes deep red when fully hydrated. For the partially hydrated sample, the broad Raman bands observed are very different from the bands observed for the fully hydrated and dehydrated

Table 1. Predicted and observed hydrated surface vanadium oxide species on different oxide supports^{28,29}

Oxide support	Net pH at PZC of oxide support	Coverage	Hydrated structures	
			Predicted	Observed
MgO	11	Low	VO ₃ (OH)	VO ₄ ^a , V ₂ O ₇ , (VO ₃) _n
		High	VO ₃ (OH), V ₂ O ₇ , (VO ₃) _n	VO ₄ ^a , V ₂ O ₇ ^a , (VO ₃) _n
Al ₂ O ₃	8.9	Low	VO ₃ (OH), (VO ₃) _n	(VO ₃) _n
		High	V ₂ O ₇ , (VO ₃) _n	(VO ₃) _n , V ₁₀ O ₂₈ ^a
ZrO ₂	5.9–6.1	Low	VO ₂ (OH) ₂ , (VO ₃) _n	V ₂ O ₇ , (VO ₃) _n ^a , V ₁₀ O ₂₈ ^a
		High	(VO ₃) _n , V ₁₀ O ₂₇ (OH)	V ₁₀ O ₂₈ ^a
TiO ₂	6.0–6.4	Low	VO ₂ (OH) ₂ , (VO ₃) _n	(VO ₃) _n ^a , V ₁₀ O ₂₈ ^a
		High	(VO ₃) _n , V ₁₀ O ₂₈	V ₁₀ O ₂₈ ^a

^a Major species.

samples.²² Therefore, the molecular structure of the surface vanadium oxide species on silica is also dependent on the degree of hydration. A combination of *in situ* Raman, UV–Vis–NIR DRS (Diffuse Reflectance Spectroscopy) and XANES spectroscopy also revealed that the structure of hydrated surface vanadium oxide species is dependent on the degree of hydration.²² Fully hydrated surface vanadium oxide species on SiO₂ closely resemble a V₂O₅·*n*H₂O gel, which is distinct from V₂O₅ crystallites.

DEHYDRATED CONDITIONS

The molecular structure of supported transition metal oxide catalysts under dehydrated conditions has been under debate in the literature for almost two decades. In particular, it was not clear how many terminal M=O bonds are present in the surface molecular entities. Transition metal oxides may possibly be present as mono-, di- or trioxo species. The combination of *in situ* Raman spectroscopy and oxygen isotopic labeling studies provides fundamental information about the number of terminal M=O bonds and, thus, discriminates between mono-, di- and trioxo species. This is illustrated schematically in Fig. 1. A monooxo species (structure A) should give rise to two strong Raman bands (M=¹⁶O and M=¹⁸O), a dioxo species (structure B) should have three strong Raman bands (¹⁶O=M=¹⁶O, ¹⁶O=M=¹⁸O and ¹⁸O=M=¹⁸O) and a trioxo species (structure C)

should give rise to four strong Raman bands (¹⁶O₃=M, ¹⁶O₂=M=¹⁸O, ¹⁶O=M=¹⁸O₂, ¹⁸O₃=M).^{33,34}

Isotopic oxygen labeling studies have allowed the determination of the molecular structures of zirconia-supported V(V), Nb(V), Cr(VI), Mo(VI), W(VI) and Re(VII) oxides.³⁵ After several reduction and reoxidation cycles, a significant extent of isotopic exchange is achieved and Table 2 shows the Raman bands of representative catalysts after calcinations with ¹⁶O₂ and after partial isotopic exchange with oxygen-18. The Raman bands of the dehydrated supported transition metal oxides after calcination in ¹⁶O₂ at 823 K in the 980–1030 cm⁻¹ range corresponds to the short terminal M=O bond (ν_s [M=O]) and the Raman bands in the 750–950 cm⁻¹ range correspond to either the anti-symmetric stretch of M–O–M bonds or the symmetric stretch of (–O–M–O–)_{*n*} bonds (ν_{as} [M–O–M] and ν_s [(–O–M–O–)_{*n*}], respectively). Isotopic substitution by oxygen-18 results in significant Raman shifts of the bands positions owing to the greater mass of oxygen-18 than oxygen-16. Both the number of the new Raman bands formed, only one additional band, and the shift to lower wavenumber values are dependent on the molecular structure of the dehydrated supported transition metal oxides (see Fig. 1) and correspond very well with the calculated values for monooxo dehydrated surface metal oxide species (structure A corresponding to one terminal bond).

Additional evidence for the monooxo structure of the supported transition metal oxides can be found from the

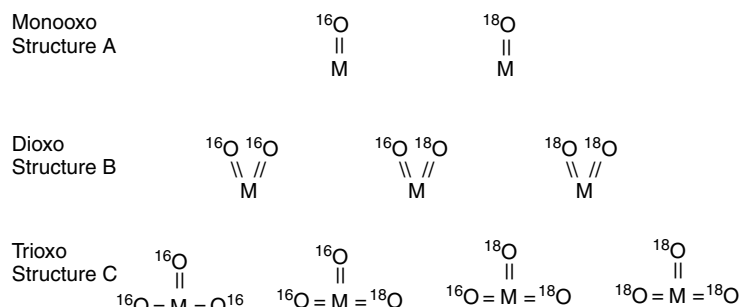


Figure 1. Schematic representation of possible structures of surface metal oxide species.

Table 2. Observed Raman bands (wavenumbers in cm⁻¹) before and after partial exchange with ¹⁸O₂³⁵

Catalyst	Experimentally observed wavenumber/cm ⁻¹	
	After calcination with ¹⁶ O ₂	After partial exchange with ¹⁸ O ₂
6% CrO ₃ /ZrO ₂	1030; 1010; 880	1030; 1010; 880; 990; 970; 840
4% MoO ₃ /ZrO ₂	996; 850	996; 850; 950(b)
5% Nb ₂ O ₅ /ZrO ₂	980; 800	980; 800; 930(b)
3% WO ₃ /ZrO ₂	1005; 790	1002; 790; 950; 750
5% V ₂ O ₅ /ZrO ₂	1030; 920	1030; 920; 990(b)
3% Re ₂ O ₇ /ZrO ₂	1005; 890	1000; 882; 945; 840

(b), Broad.

comparison of the Raman and IR bands obtained for the same catalyst under dehydrated conditions. The presence of only one vibration at the same wavenumber from Raman and IR indicates a monooxo species because a diatomic oscillating system has only one stretching mode (ν_s) since for a dioxo species two bands due to the symmetric (ν_s) and antisymmetric (ν_{as}) stretching modes will be visible.^{33,34} These wavenumbers should be separated by ca 20 cm^{-1} . Furthermore, for dioxo species the symmetric mode will be more intense in Raman, while the antisymmetric mode will dominate in IR. A more complex situation should occur for a trioxo species. Based on the coincident values of the IR and Raman wavenumbers it appears that the supported transition metal oxides are present as surface monooxo species.³⁶

The dehydrated monooxo species can be present as either surface isolated or polymerized structures, where dehydrated polymeric species also possesses bridging M—O—M bonds that can be detected at ~ 900 (antisymmetric stretch), 600 (symmetric stretch) and 200 (bending mode) cm^{-1} . Thus, molybdena on zirconia is present as a surface polymeric monooxo species because of the Raman vibrations at 996 (Mo=O symmetric stretch) and 850 cm^{-1} (Mo—O—Mo antisymmetric stretch). The structural information can be further complemented by other techniques, such as XANES, that reveal that Mo has a formal coordination of five, which is close to a distorted octahedral coordination.²⁷ Similar structures can be envisioned also for the dehydrated surface tungsten oxide and niobia species. A surface polymeric species occurs for surface vanadia species on ZrO_2 , which possesses a pseudo-tetrahedral coordination, giving rise to Raman vibrations near 1030 (terminal V=O) and 920 (bridging V—O—V) cm^{-1} .³⁵ The coordination model for rhenium oxide on zirconia is proposed as a surface polymeric species, in which at least two octahedron-like coordinated Re^{7+} atoms are linked via an oxygen atom, one terminal Re=O bond and four bridging Re—O—Zr bonds.³⁵

The Raman study of the dehydrated catalysts does not provide any indication as to which of the Raman bands of the terminal M=O bond corresponds to the surface isolated or polymeric species. However, *in situ* reactivity studies under reducing conditions³⁷ have shown that the Raman bands due to the surface isolated and polymeric species can be discriminated by their different reduction activity. For example, supported polymeric chromium oxide species are more reducible than the isolated species and reveal that the terminal M=O bond of dehydrated isolated monooxo species are characterized by a Raman band at a higher wavenumber (1030 cm^{-1}) than that of the dehydrated polymeric monooxo species (1010 cm^{-1}). In the case of the silica support, only dehydrated monochromate surface species are observed.³⁷ For vanadium oxide supported on CeO_2 , the terminal V=O mode of the dehydrated isolated surface vanadium oxide occurs at 1034 cm^{-1} and that of the dehydrated polymeric vanadium oxide species is observed

at 1017 cm^{-1} .³⁸ Similar observations have also been made for molybdenum oxide, tungsten oxide and rhenium oxide supported on CeO_2 .³⁹ In the case of the silica support, only dehydrated isolated surface metal oxide species are observed.

The terminal M=O bond and the bridging M—O—M bonds are detectable by Raman spectroscopy; however, the bridging M—O—support bonds are not detectable by Raman spectroscopy since they are too ionic to be Raman active. The study of the bridging M—O—support bonds cannot be done directly by Raman spectroscopy. For $\text{V}_2\text{O}_5/\text{TiO}_2/\text{SiO}_2$, however, where a bilayer of surface vanadia layer on a surface titania layer on silica is present, the bridging V—O—Ti bonds have been directly detected with Raman spectroscopy.²⁴ Other characterization techniques can provide additional structural information about the local environment of the different metal cations, solid-state NMR, XANES/EXAFS and UV-Vis revealed that both the coordination of the surface vanadia species and the surface titania species are altered by the formation of the bridging V—O—Ti bond between the two layers.²⁴

WET OXIDATION

Supported metal oxide catalysts under ambient conditions are extensively hydrated owing to the presence of significant amounts of adsorbed moisture at room temperature. The adsorbed moisture has a pronounced effect on the molecular structures of the surface metal oxide phases and the situation in aqueous environments has already been described (see above). Under *in situ* dehydrated conditions, the adsorbed moisture desorbs upon heating and the surface metal oxide species becomes dehydrated. The molecular structures of the dehydrated supported metal oxides have also been described above. However, water vapor is usually present in the feed gas or as a reaction product in many catalytic reactions at elevated temperatures. The presence of significant amounts of water vapor can affect the extent of surface hydroxylation, the ratio of Brønsted-to-Lewis surface acid sites or the molecular structures of the surface metal oxide species, which can have a significant effect on many reactions over supported metal oxide catalysts.

A detailed fundamental study on the nature of supported vanadium oxide catalysts at high temperature in the presence of water vapor was recently reported.⁴⁰ This is illustrated in Fig. 2 for surface vanadium oxide species on an Al_2O_3 support. For 4% $\text{V}_2\text{O}_5/\text{Al}_2\text{O}_3$, the Raman band of the terminal V=O bond of the surface vanadium oxide species shifts from 1012 to 1003 cm^{-1} on decreasing the catalyst temperature from 773 to 443 K and simultaneously becomes broad in the presence of moisture. However, the bridging V—O—V functionality of the surface vanadia species on alumina (900–800, 620–450 and 350–200 cm^{-1}) appears to be only modestly influenced by the presence of adsorbed water vapor, which is primarily related to the broadness

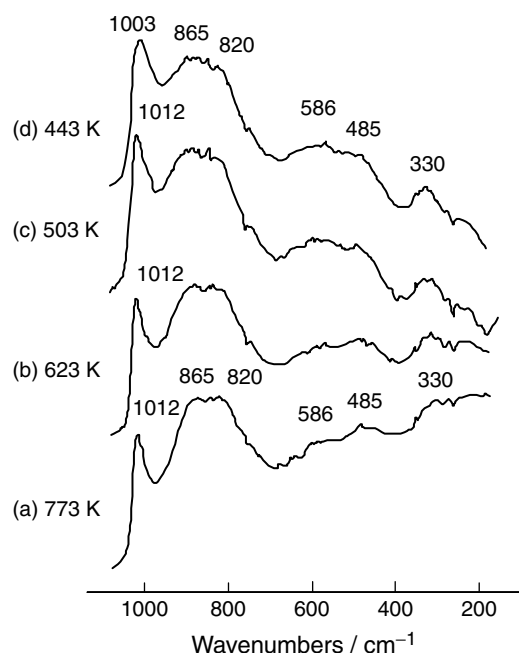


Figure 2. *In situ* Raman spectra of 4% V_2O_5/Al_2O_3 in the presence of water vapor at various temperatures.

on this band relative to the sharper Raman band for the terminal $V=O$ bond. Similar trends are observed for surface vanadium oxide species supported on titania and ceria (Table 3). However, silica-supported vanadium oxide only shows a very moderate change in the Raman band position of the terminal $V=O$ bond from 1038 to 1032 cm^{-1} on increasing temperature in a moist environment, owing to the

hydrophobic nature of the silica surface and thermal effects on the length of the $V-O$ terminal bond with temperature.⁴¹ In general, at low surface vanadium oxide coverage and high temperatures (573 K and above), the presence of water vapor has no appreciable effect on the terminal $V=O$ Raman bands in the $1018\text{--}1038\text{ cm}^{-1}$ region. Thus, the molecular structures of the surface metal oxide species under flowing moisture and elevated temperatures are essentially the same as those for the corresponding dehydrated surface metal oxide species already discussed above.

Isotopic oxygen exchange studies with $H_2^{16}O/^{16}O_2$ on an oxygen-18-labeled 4% V_2O_5/ZrO_2 catalyst⁴⁰ indicate that the surface vanadia species undergoes oxygen exchange with moisture in a few minutes at 573 K and 8% H_2O , whereas exchange is not efficient with just dry $^{16}O_2$. The origin of this different oxygen exchange behavior between water vapor and oxygen is related to the ability of moisture to hydrogen bond to the oxygen functionalities of the surface vanadia species ($V=O$, $V-O-V$ and $V-O\text{---}support$). The hydrogen bonding is directly observed for the terminal $V=O$ bond since the shift of this sharp Raman band to lower wavenumbers is very evident. However, the broad Raman bands of the bridging $V-O-V$ bonds do not allow for such a precise evaluation. The formation of solvated surface vanadia species at lower temperatures (below 503 K) reveals that moisture is also able to hydrolyze the $V-O\text{---}supported$ bonds. However, at elevated temperatures (above 503 K), the hydrolysis reaction does not appear to occur to a significant extent and the surface vanadia species are stable on the oxide supports in the presence of moisture. Thus, moisture is able to interact with the oxygen functionalities of the fully

Table 3. Effect of water vapor at elevated temperatures on the Raman bands of surface vanadia species on oxide supports⁴⁰

Catalyst	Conditions	Stretching mode/ cm^{-1}		Bending mode/ cm^{-1}	
		$V=O$	$V-O-V$	$V-O$	$V-O-V$
1% V_2O_5/SiO_2	Vapor, 503 K	1038	—		
	Dehydrated	1038	—		
7% V_2O_5/SiO_2	Vapor, 503 K	1037	—		
	Dehydrated	1037	—		
1% V_2O_5/TiO_2	Vapor, 503 K	1018	920		
	Dehydrated	1028	920		
5% V_2O_5/TiO_2	Vapor, 503 K	1029	920		
	Dehydrated	1030	920		
1% V_2O_5/CeO_2	Vapor, 503 K	1012	920		
	Dehydrated	1023	920		
3% V_2O_5/CeO_2	Vapor, 503 K	1018	900		
	Dehydrated	1026	920		
4% V_2O_5/Al_2O_3	Vapor, 503 K	1018	865, 820, 586, 485	330	
	Dehydrated	1018	875, 800, 600	330	
18% V_2O_5/Al_2O_3	Vapor, 503 K	1013	900, 800, 615, 530, 460	330	240
	Dehydrated	1027	900, 800, 615, 530, 460	330	240

oxidized surface vanadia species via hydrogen bonding, but the structural transformations in the presence of moisture are only observed at low temperatures (below 503 K).

The ability of moisture to interact with the surface vanadia species at elevated temperatures implies that moisture competitively adsorbs with the reactants on such surface adsorption sites during oxidation reactions. Thus, the rate of oxidation reactions over supported vanadia catalysts should generally decrease in the presence of moisture and this effect should increase with decreasing reaction temperature. This is in line with literature studies on the effect of moisture upon the selective catalytic reduction of NO_x with NH_3 over $\text{V}_2\text{O}_5/\text{TiO}_2$ catalysts. All of these studies demonstrate that the presence of moisture decreases the conversion of NO and that the effect of moisture becomes more pronounced at lower reaction temperatures.⁴² In addition, the selectivity towards undesirable N_2O formation is suppressed by the presence of moisture, which has been attributed to surface hydroxylation.^{42–44} In fact, *in situ* IR studies during SCR (Selective Catalytic Reduction) over vanadia/titania catalysts show that moisture adsorbs via hydrogen bonds, increases the surface hydroxyl concentration and coordinates to the surface vanadia species.⁴³

OXIDATION REACTIONS CONDITIONS

C_2 – C_4 alkanes (LPG) oxidation reaction conditions

Butane oxidation to maleic anhydride was investigated over supported vanadia/alumina.⁴⁵ The Raman spectrum of the fully oxidized, dehydrated system exhibits bands at 920, 800, 600 and 550 cm^{-1} due to the presence of bridging V—O—V bonds and 1028 cm^{-1} due to the terminal V=O bonds. During *n*-butane oxidation, the polymeric V—O—V functionalities are preferentially reduced relative to the terminal V=O bonds. This trend becomes more evident as the reaction temperature increases. In the absence of oxygen, both the terminal V=O and the bridging V—O—V bonds are absent from the *in situ* Raman spectrum owing to extensive reduction of the surface vanadia sites. Unfortunately, the reduced surface vanadia species does not give rise to new Raman bands owing to its very weak or inactive Raman signal (most likely because of the absence of the V=O functionality, which gives rise to a strong Raman signal). Exposure to an oxygen environment reoxidizes the surface vanadia species and yields the initial Raman spectrum of the fresh catalysts.⁴⁵ Essentially the same trends were observed with vanadia supported on titania, zirconia, niobia, ceria and binary oxide supports such as $\text{P}_2\text{O}_5/\text{TiO}_2$. Thus, the surface vanadia species on oxide supports reduces partially during *n*-butane oxidation and the bridging V—O—V functionality is preferentially reduced relative to the terminal V=O bond.^{45,46}

The extent of reduction of supported vanadium oxide species depends on the reactivity of the hydrocarbon. Thus, reduction is less evident during the selective oxidation of

propane and ethane for the same catalytic systems; only 4% $\text{V}_2\text{O}_5/\text{ZrO}_2$ shows some reduction of the polymeric V—O—V functionalities.^{47–49} Other *in situ* techniques provide complementary information about the states of the supported vanadium oxide species under reaction conditions for butane and ethane selective oxidation reactions.^{47,50} The complementary study by *in situ* UV–Vis DRS⁵⁰ on supported vanadium oxide catalysts shows that the extent of reduction of supported vanadium oxide is higher under *n*-butane oxidation than under ethane oxidation. In particular, the extents of reduction of V(V) sites determined by *in situ* UV–Vis DRS for 1% $\text{V}_2\text{O}_5/\text{ZrO}_2$ and 4% $\text{V}_2\text{O}_5/\text{ZrO}_2$ are ca 2.8 and 3.6% under ethane oxidation, ca 1.8 and 8.2% under propane oxidation and ca 8.0 and 9.6% under butane oxidation.⁵⁰ This is consistent with the expected reactivity of the C_2 – C_4 alkanes, determined by the weakest C–H bond, and the trends observed by *in situ* Raman reaction studies with the same C/O atomic ratio in the hydrocarbon/ O_2 /He feed.^{44–50}

Role of the terminal V=O bond

The butane turnover frequency (TOF) is a strong function of the specific oxide support and varies by a factor of ~ 50 (titania > ceria > zirconia > niobia > alumina > silica), but does not correspond with the changes in the position of the terminal V=O bond.⁴⁵ A lack of such a correlation was also found for ethane oxidation on supported-vanadia catalysts.²⁰ The *in situ* Raman spectra of the oxygen-18 exchanged 2% $\text{V}_2\text{O}_5/\text{SiO}_2$ and 10% $\text{V}_2\text{O}_5/\text{Al}_2\text{O}_3$ during ethane oxidation reaction conditions are illustrated in Fig. 3. Each supported-vanadia catalyst initially shows a Raman band at 1031 or 1017 cm^{-1} that corresponds to the terminal $\text{V=}^{16}\text{O}$ vibrations of the dehydrated surface vanadia on silica and alumina, respectively. New Raman bands appear near 988 and 976 cm^{-1} upon exchange with $^{18}\text{O}_2$ that correspond to the terminal $\text{V=}^{18}\text{O}$ vibrations on silica and alumina, respectively. These wavenumber shifts quantitatively correspond with the predicted values from the change in the reduced mass of the V—O bond when oxygen-16 is replaced with oxygen-18. Alumina-supported vanadia exhibits a very broad Raman band at $\sim 860\text{ cm}^{-1}$, due to the bridging V—O—V bond. A weak shoulder at $\sim 900\text{ cm}^{-1}$ is evident after oxygen-18 exchange, which corresponds to the vibration of the exchanged $\text{V—}^{18}\text{O—V}$ bond. The *in situ* Raman spectra in Fig. 3 for $\text{V}_2\text{O}_5/\text{Al}_2\text{O}_3$ and $\text{V}_2\text{O}_5/\text{SiO}_2$ show that the supported vanadia species is essentially not reduced during ethane oxidation. The Raman intensities of the 988 and 1031 cm^{-1} bands of the 2% $\text{V}_2\text{O}_5/\text{SiO}_2$ catalyst are monitored as a function of time-on-stream during ethane oxidation with $^{16}\text{O}_2$ [Fig. 3(A)]. The Raman band of the terminal $\text{V=}^{18}\text{O}$ bond decreases rather fast during the first minutes under reaction conditions at 863 K; however, it is not fully exchanged, even after more than 11 min time-on-stream, which corresponds to about eight catalytic cycles. The exchanged 10% $\text{V}_2\text{O}_5/\text{Al}_2\text{O}_3$ shows a similar behavior

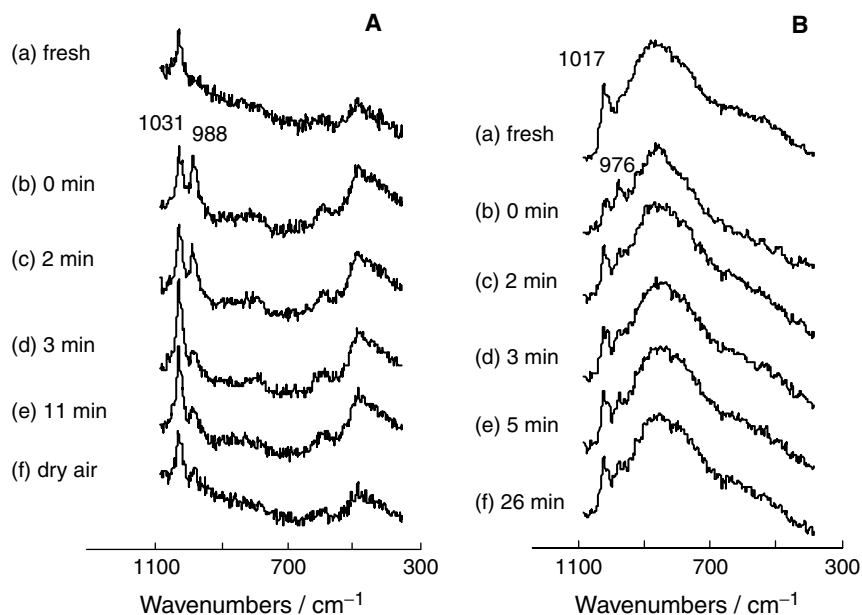


Figure 3. Reaction *in situ* (operando) Raman spectra of partially oxygen-18-exchanged supported vanadia catalysts under ethane oxidation reaction conditions: (A) 2% V_2O_5/SiO_2 at 863 K ($TOF = 1.2 \times 10^{-2} s^{-1}$); (B) 10% V_2O_5/Al_2O_3 at 783 K ($TOF = 6.9 \times 10^{-3} s^{-1}$).

[Fig. 3(B)]; the intensity of the $V=O^{18}$ Raman band is weak but still evident even after 26 min on-stream, which corresponds to ~ 11 catalytic cycles. If the terminal $V=O$ bond were involved in the rate-determining step, it should be exchanged within one catalytic cycle. Consequently, the terminal $V=O$ bond must not be the kinetically critical active site of the supported-vanadia catalysts since it is not fully exchanged within ~ 10 catalytic cycles.

In addition, *in situ* Raman experiments with oxygen-18 labeling of the terminal $V=O$ bond during butane oxidation showed that the exchange time of this bond was ca 20 times longer than the characteristic reaction time ($1/TOF$).⁴⁶ The same effect has also been observed for the oxidation of methane to formaldehyde.⁵¹ All these studies suggest that the terminal $V=O$ bond is too stable to be involved in the rate-determining step of these alkane oxidation reactions. This is in agreement with preliminary studies where no correlation was found between the terminal $V=O$ bond Raman band position, or bond strength, and the catalytic TOF value.²⁰ On the other hand, the strong influence of the specific oxide support ligands on the butane oxidation TOF (a factor of ~ 50) suggests that the bridging $V-O$ -support bonds are involved in the kinetically critical rate-determining step associated with *n*-butane oxidation (activation of an internal C—H bond).

Coverage effect and the role of the bridging $V-O-V$ bond

The surface coverage of an active metal oxide on an oxide support increases the surface polymeric to isolated population ratio, as revealed by *in situ* Raman and UV-Vis

spectra. The relevance that it may have on catalytic performance can be evaluated from its influence upon the TOF values. The $V-^{18}O-V$ bond appears to exchange faster than the terminal $V=^{18}O$ bond (see Fig. 3); hence it appears that the bridging $V-O-V$ bond may have a more prominent role than the terminal $V=O$ bond. However, its relevance must be moderate since any increase in surface vanadia coverage on an alumina support has only a minor effect on the TOF of ethane oxidation to ethylene ($4.4 \times 10^{-3} s^{-1}$ for 5% V_2O_5/Al_2O_3 and $4.0 \times 10^{-3} s^{-1}$ for 15% V_2O_5/Al_2O_3 at 803 K).⁴⁷ Also, surface vanadia coverage on zirconia also shows no significant effect on the TOF values of propane oxidation to propylene ($4.4 \times 10^{-3} s^{-1}$ for 1% V_2O_5/ZrO_2 and $4.0 \times 10^{-3} s^{-1}$ for 2% V_2O_5/ZrO_2).^{11,48} Thus, ethane and propane oxidative dehydrogenation (ODH) show little change in their TOF values upon increasing the surface vanadia coverage on several different oxide supports.^{47–49} Consequently, ethane and propane oxidative dehydrogenation TOF values are not influenced to any appreciable extent by the surface concentration of polymeric $V-O-V$ functionalities, which increase with the surface vanadia coverage. Furthermore, the relatively constant TOF values with surface vanadia coverage reveals that the oxidative dehydrogenation of ethane and propane to their corresponding olefins requires only one surface vanadia site. However, the TOF values for *n*-butane oxidation to maleic anhydride increase with increasing surface vanadia coverage indicating that adjacent surface vanadia sites are more efficient in selectively oxidizing *n*-butane to maleic anhydride than the isolated surface vanadia sites.^{45,46} This is not surprising since the oxidation of *n*-butane to maleic anhydride requires the involvement

of four oxygen atoms [each surface vanadia site can only contribute one oxygen atom since the maximum reduction is from V(V) to V(III), assuming that gas-phase oxygen does not directly participate (Mars–van Krevelen mechanism)]. Therefore, the specific requirements of the reactant and its corresponding product, rather than the ratio of polymeric to isolated surface vanadia species, determine the relevance of the surface metal oxide coverage.

Support effect

The selectivity to maleic anhydride during *n*-butane oxidation depends strongly on the specific oxide support: $\text{Al}_2\text{O}_3 > \text{Nb}_2\text{O}_5 > \text{TiO}_2 > \text{SiO}_2 > \text{ZrO}_2 > \text{CeO}_2$. This trend parallels the strength of the Lewis acidity of the oxide support. Alumina has the strongest Lewis acid sites, followed by niobia, and the other supports have weak (titania and zirconia) or no Lewis acid sites (silica).⁵² This observation is consistent with the critical reaction step involving the bridging V—O—support bond, which is in immediate vicinity of the Lewis acid sites of the oxide support.

The TOF values for *n*-butane oxidation to maleic anhydride^{45,46} and for the ethane ODH (Oxidative Dehydrogenation) to ethylene over supported vanadium oxide catalysts²⁰ also depend strongly on the specific oxide support. Ethane ODH TOF values change by more than an order of magnitude ($\text{TiO}_2 > \text{ZrO}_2 \gg \text{Al}_2\text{O}_3 > \text{Nb}_2\text{O}_5 > \text{CeO}_2 > \text{SiO}_2$) and those for *n*-butane oxidation change by a factor of 50 ($\text{TiO}_2 > \text{CeO}_2 > \text{ZrO}_2 > \text{Nb}_2\text{O}_5 > \text{Al}_2\text{O}_3 > \text{SiO}_2$). With the exception of the vanadia/ceria catalytic system, which

undergoes solid-state reaction and decreases the number of surface vanadia active sites, the TOF values for *n*-butane oxidation increase with decreasing electronegativity of the oxide support (the more basic bridging V—O—S bonds are more efficient in activating the internal C—H bonds). The dependence of the TOF values for *n*-butane oxidation also parallels the reducibility trend of the surface vanadium oxide species on these supports, which is most probably just coincidental. However, the ethane ODH TOF values show some deviation from this trend owing to solid-state reactions between the surface vanadia and the ceria and niobia supports at the much higher reaction temperatures required for ethane activation. This issue will be discussed further in the section below on structural transformations under different environments.

Methane oxidation reaction conditions

The *in situ* Raman spectra of $\text{MoO}_3/\text{SiO}_2$ catalysts under methane oxidation reaction conditions reveal that the surface molybdate oxide species possesses the same molecular structure as the dehydrated surface molybdenum oxide species on silica [Fig. 4(A)].⁵³ The effect of alkali metal cations addition on the structure and performance of $\text{MoO}_3/\text{SiO}_2$ catalysts for the partial oxidation of methane and methanol has been investigated.⁵³ It was shown that the alkali metal cations cause a decrease in the number of isolated surface Mo oxide species, possessing one terminal Mo=O bond and four bridging Mo—O—Si bonds, by the formation of alkali metal–molybdate compounds. Consequently, the

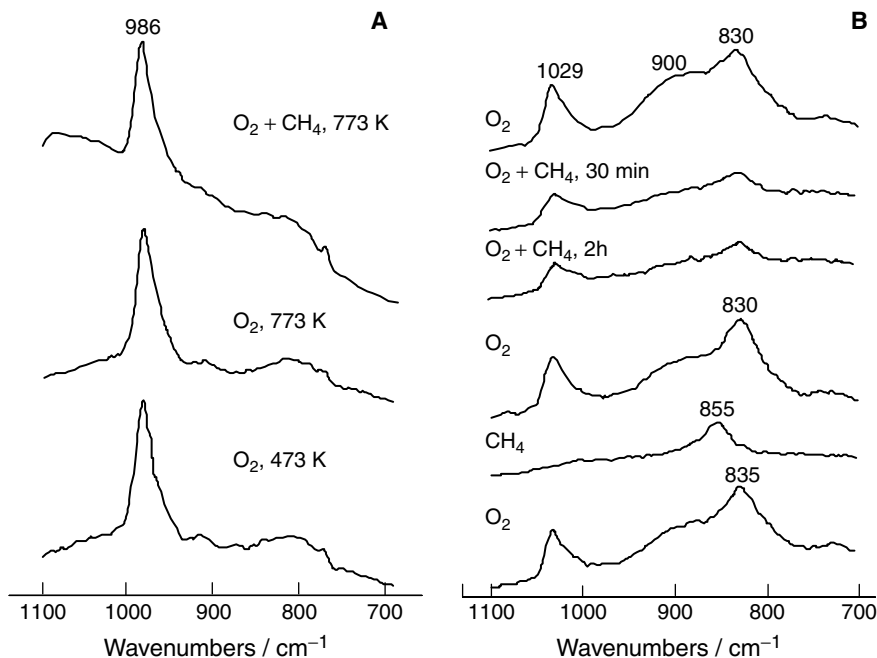


Figure 4. Reaction *in situ* Raman spectra of 5% $\text{MoO}_3/\text{SiO}_2$ dehydrated and under methane oxidation reaction conditions (operando) (A); and *in situ* (operando) Raman spectra of 1% $\text{V}_2\text{O}_5/\text{SnO}_2$ at 773 K under sequential treatments in flowing O_2 , CH_4/O_2 (10 : 1) reactant mixture and CH_4 (B).

catalytic activity for methane oxidation to formaldehyde over the $\text{MoO}_3/\text{SiO}_2$ catalyst is decreased since the number of isolated surface Mo oxide active species is reduced. When both surface vanadium and molybdenum oxides are supported on silica, both species are isolated and co-exist over the silica support without any interactions and the catalytic performance is dominated by the more active surface vanadium oxide species.⁵⁴

In situ Raman studies of $\text{V}_2\text{O}_5/\text{SiO}_2$, $\text{V}_2\text{O}_5/\text{TiO}_2$ and $\text{V}_2\text{O}_5/\text{SnO}_2$ and $\text{V}_2\text{O}_5/\text{TiO}_2/\text{SiO}_2$ demonstrate that the dehydrated surface vanadia species exhibits a sharp Raman band at $\sim 1027\text{--}1034\text{ cm}^{-1}$ from the terminal $\text{V}=\text{O}$ bond, while the surface bridging $\text{V}-\text{O}-\text{V}$ polymeric species exhibit a broad Raman band $\sim 900\text{ cm}^{-1}$ on the SnO_2 and TiO_2 supports. In addition, the SnO_2 system shows a new band near 830 cm^{-1} , associated with a bulk $\text{V}-\text{Sn}-\text{O}$ compound.⁵⁴ Under methane oxidation reaction conditions, the Raman intensities of the surface vanadium oxide species decreases for the supported $\text{V}_2\text{O}_5/\text{TiO}_2$ and $\text{V}_2\text{O}_5/\text{SnO}_2$ catalytic systems owing to the reduction of the surface vanadium oxide species under the reducing methane oxidation environment, but no significant changes were observed for the $\text{V}_2\text{O}_5/\text{SiO}_2$ and $\text{V}_2\text{O}_5/\text{TiO}_2/\text{SiO}_2$ systems. In the case of the SnO_2 -supported vanadia catalyst, reduction resulted in a reduced surface V(IV) or V(III) phase characterized by a weak and broad Raman band at 855 cm^{-1} [Fig. 4(B)].

Similar to the oxidation of the $\text{C}_2\text{--C}_4$ alkanes, the oxygen in the terminal $\text{V}=\text{O}$ bond does not appear to be the critical site for methane oxidation. Oxygen isotopic studies show that the terminal $\text{V}=\text{O}$ bond in the $\text{V}_2\text{O}_5/\text{SiO}_2$ catalyst is too stable under the reaction conditions to be the kinetically critical active site for activating the $\text{C}-\text{H}$ bond in methane.⁵¹ However, the catalytic data do show that the overall methane oxidation activity is dependent on the specific oxide support. The $\text{V}-\text{O}$ -support bond strength must vary with the support and is most probably responsible for the different catalytic TOF values observed over these supported vanadium oxide catalytic systems. It is also possible that some surface V(V) species will be reduced and provide sites for oxygen adsorption to form electrophilic oxygen species.⁵⁵ The population of the reduced surface vanadia species depend on the specific catalyst support since the *in situ* Raman spectra show that the reduced species are not present over the SiO_2 support and are much more prevalent over titania and SnO_2 supports under the reaction conditions employed. The extent of reduction of the surface vanadium species oxide follows the trend $\text{SnO}_2 > \text{TiO}_2 > \text{SiO}_2$, which correlates with the CO_2 selectivity and inversely with the formaldehyde selectivity. The CO product arises from the direct decomposition of the formaldehyde intermediate product and CO_2 arises from the direct combustion of methane and further oxidation of CO.

SCR (NO and NH_3) reaction conditions

The *in situ* Raman spectra of the supported vanadium oxide catalysts for the selective catalytic reduction (SCR) of NO with NH_3 reveal that increasing the surface vanadia coverage increases the ratio of polymerized to isolated surface vanadia species, the same Raman spectra are obtained under dehydrated and SCR reaction conditions. Corresponding IR studies, employing NH_3 adsorption, demonstrated that the number of surface Brønsted acid sites also increases with increasing surface vanadia coverage. The SCR De NO_x TOF values were found to increase with surface vanadia coverage, but the specific redox properties of the surface vanadia species were not affected. The increasing SCR TOF with surface vanadia coverage reveals that the bimolecular NO and NH_3 SCR reaction requires more than one surface site. This suggests that the immediate environment of the surface redox site is critical. This could originate from the need for two adjacent surface redox sites, a surface redox site adjacent to an acid site or to the higher activity of polymerized surface vanadia species relative to that of isolated surface vanadia species. However, it is not straightforward to discriminate among these different possibilities from the surface vanadia coverage effect on the SCR reaction. The addition of surface tungsten oxide and niobium oxide species to a 1% $\text{V}_2\text{O}_5/\text{TiO}_2$ catalyst increases the SCR TOF by up to an order of magnitude, with the surface tungsten oxide somewhat more efficient than the surface niobium oxide species. Surface NbO_x (Lewis acid) and WO_x (Brønsted acid) do not possess redox properties. Thus, the De NO_x reaction does not necessarily require two adjacent surface redox sites (isolated or polymeric). Nor does the introduction of these acidic promoters alter the ratio of polymerized to isolated surface vanadia species to any appreciable extent, but the SCR TOF values increase with the introduction of the acidic surface additives. The presence of surface WO_x or NbO_x promoters increases the presence of surface Brønsted or Lewis acid sites, respectively. Ammonia initially adsorbs on the surface acid sites and reduces the adjacent surface vanadia species from V(V) to V(III), which creates a vacancy for the adsorption of NO_x [NO_x does not adsorb on surface V(V) sites]. The adjacent chemisorbed NO_x and NH_x species then combine to form the desired N_2 and H_2O reaction products. The reduced surface vanadia sites are then rapidly reoxidized by gas-phase oxygen. Thus, the SCR reaction is most efficient in the presence of adjacent surface redox and surface acid sites ($\text{WO}_x > \text{VO}_x > \text{NbO}_x$).⁵⁶

The reaction *in situ* Raman spectra of 4% $\text{V}_2\text{O}_5/\text{ZrO}_2$ during the SCR reaction at 573 K are presented in Fig. 5. The catalyst was partially exchanged with oxygen-18 via a series of successive *n*-butane reduction and $^{18}\text{O}_2$ oxidation cycles. The heavier mass of oxygen-18 relative to oxygen-16 shifts the Raman band from ~ 1030 to $\sim 990\text{ cm}^{-1}$ (Fig. 5). The time required to exchange the terminal $\text{V}=\text{O}$ bond to $\text{V}=\text{O}^{18}$ during the SCR reaction (containing only $^{16}\text{O}_2$, N^{16}O and NH_3) was monitored by *in situ* Raman spectroscopy.

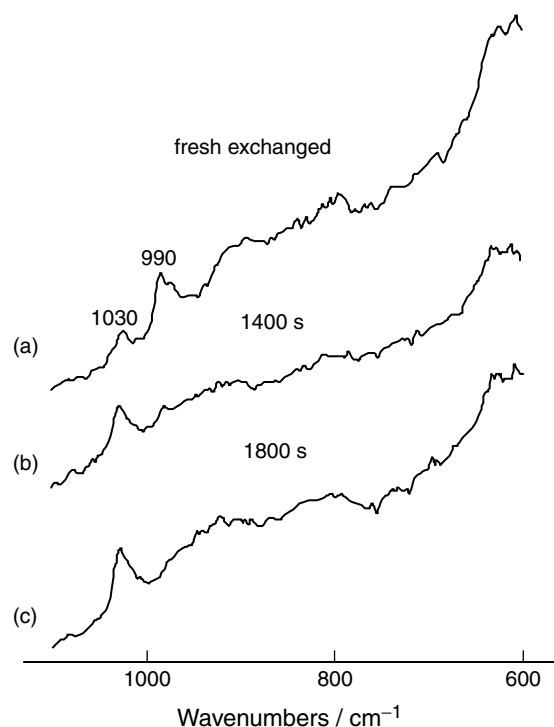


Figure 5. Reaction *in situ* (operando) Raman spectra of 4% V_2O_5/ZrO_2 during SCR reaction at 573 K. (a) Partially exchanged with $^{18}O_2$; (b) after SRC of NO with NH_3 for 1400 s; (c) After SRC of NO with NH_3 for 1800 s.

The exchange process took ~ 1800 s to complete and the SCR characteristic reaction time ($1/TOF$) was ~ 180 s. This reveals that it took nearly 10 reaction cycles to exchange the isotopically labeled $V=^{18}O$ terminal bond completely. Therefore, the terminal $V=O$ bond is too stable to be directly involved in the rate-determining step for the SCR reaction. The *in situ* Raman spectra also reveal that the molecular structure of the supported metal oxides under SCR reaction conditions is the same as the surface metal oxides under dehydrated conditions. The active surface sites for SCR $DeNO_x$ reaction are also influenced by the oxide support since the TOF values vary by a factor of 6 at 473 K⁵⁶ ($ZrO_2 > TiO_2 \gg Al_2O_3 > SiO_2$), which correlates with the reduction in the electronegativity of the support cation ($Zr < Ti < Al < Si$). Thus, the bridging $V-O$ -support bond also appears to be involved in the kinetic critical rate-determining step during the SCR reaction. This conclusion is consistent with model SCR studies with unsupported V_2O_5 crystals that reported that the crystallographic planes possessing bridging $V-O-V$ or $V-OH$ bonds rather than terminal $V=O$ bonds were the active sites for the SCR reaction.^{57,58}

Methanol oxidation reaction conditions

The molecular structures of surface vanadium oxide species supported on different oxide supports during methanol

oxidation have been investigated with *in situ* Raman spectroscopy.^{36,59,60} Supported vanadium oxide species are stable during methanol oxidation, but some differences are also evident. Upon introduction of a methanol/ O_2 /He gas stream both the terminal $V=O$ and bridging $V-O-V$ Raman bands decrease in intensity and shift to lower wavenumbers for all the supported vanadia catalysts. The decrease in intensity and downward shift of the Raman bands is more pronounced for lower reaction temperature (503 K) than for the higher reaction temperatures (573–633 K). The bridging $V-O-V$ Raman band at ~ 950 cm^{-1} also decreases in intensity during methanol oxidation and the maximum of this broad feature shifts towards ~ 920 cm^{-1} . *In situ* UV-Vis DRS spectra under the same reaction conditions exhibit a change in the coordination rather than a reduction of the surface $V(V)$ species during the methanol oxidation reaction.³⁷ Only surface vanadia on alumina and zirconia show a moderate extent of reduction during methanol oxidation. If the changes caused during methanol oxidation reaction were due to the reduction of surface $V(V)$ species, it would have been more severe at high conversions upon increasing the temperature (which is not the case). Thus, the downward shift in vibrational wavenumber of the terminal $V=O$ Raman band is consistent with a lengthening of the $V=O$ bond by coordination or H-bonding to chemisorbed methoxy species or water (see the above section on wet oxidation). Thus, supported metal oxides under methanol oxidation reaction conditions tend to be oxidized and possess molecular structures similar to those found under dehydrated conditions.

In situ Raman studies of supported transition metal oxide catalysts under methanol oxidation conditions have been measured for different supported metal oxides (V, Nb, Cr, Mo, W and Re) on different oxide supports (SiO_2 , CeO_2 , CeO_2/SiO_2 , ZrO_2 , TiO_2 , Nb_2O_5 and Al_2O_3).^{37,59–63} For silica-supported vanadium oxide, stable surface methoxy species form via reaction with the surface silanol groups. The *in situ* Raman experiments during methanol oxidation reveal that both surface $Si-OCH_3$ as well as surface $V-OCH_3$ species are formed. The $V-OCH_3$ species exhibit Raman bands at 1067 cm^{-1} (C–O vibration in $VO-CH_3$) and 665 cm^{-1} ($V-O-CH_3$ vibrations) [Fig. 6(A)]. In addition, the intensity of the Raman bands due to $V-OCH_3$ methyl vibrations at 2930 and 2830 cm^{-1} increase their intensity with respect to those of the $Si-OCH_3$ vibrations at 2960 and 2860 cm^{-1} as the surface vanadium oxide coverage increases [Fig. 6(B)]. The number of available surface $Si-OH$ sites for methanol chemisorption decreases with increasing surface vanadium oxide loading because the surface vanadium oxide species titrates the exposed surface $Si-OH$ sites. The Raman bands for the different surface metal oxide species on silica during methanol oxidation are summarized in Table 4. Stable surface $M-OCH_3$ species are only found on the V_2O_5/SiO_2 system (Raman bands near 1070 and 660 cm^{-1}). For other silica-supported oxides, the surface

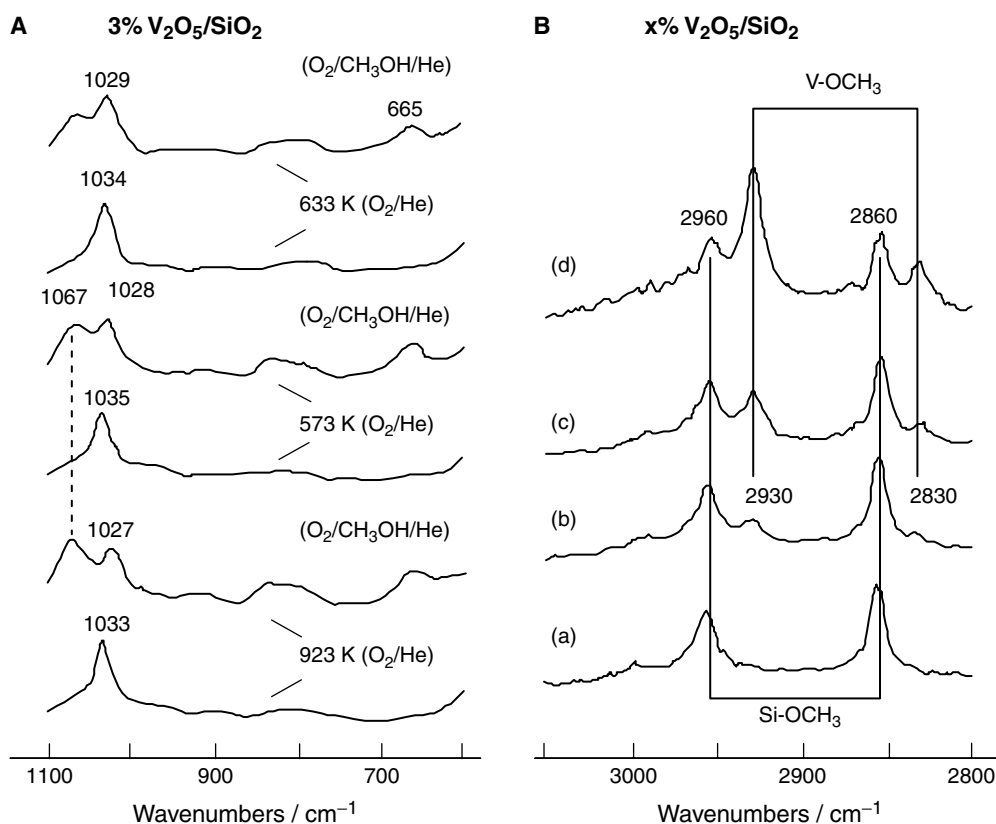


Figure 6. *In situ* Raman spectra in the metal–oxygen stretching region of 3% V_2O_5/SiO_2 under O_2 or $CH_3OH/O_2/He$ flow at different temperatures (A). *In situ* Raman spectra in the C–H stretching region of V_2O_5/SiO_2 catalysts under $CH_3OH/O_2/He$ flow at 503 K (B). (a) 0% V_2O_5/SiO_2 (b) 1% V_2O_5/SiO_2 (c) 3% V_2O_5/SiO_2 (d) 7% V_2O_5/SiO_2 .

Table 4. Raman wavenumbers (cm^{-1})^a of the surface methoxy species on a silica support⁵⁹

Catalyst	Si—OCH ₃ (asym C—H)	Si—OCH ₃ (sym C—H)	M—OCH ₃	Si—OCH ₃ (sym C—H)	M—OCH ₃
SiO ₂	2990 (w)	2958 (s)		2856 (s)	
1% V_2O_5/SiO_2	2990 (w)	2957 (s)	2931 (m)	2857 (s)	2834 (m)
7% V_2O_5/SiO_2		2954 (m)	2930 (s)	2854 (m)	2832 (m)
1% Nb_2O_5/SiO_2		2954 (s)		2856 (s)	
5% Nb_2O_5/SiO_2		2956 (vw)		2856 (vw)	
1% Cr_2O_3/SiO_2	— ^b	— ^b	— ^b	— ^b	— ^b
1% MoO_3/SiO_2	2995 w	2957 (s)		2857 (s)	
5% MoO_3/SiO_2	2995 w	2957 (s)		2857 (s)	
3% WO_3/SiO_2		2957 (s)		2857 (s)	
1% Re_2O_7/SiO_2		2956 (s)		2856 (s)	
5% Re_2O_7/SiO_2		2956 (s)		2856 (s)	

^a w, Weak; s, Strong; m, Medium; v, Very.

^b Fluorescence under methanol oxidation reaction.

methoxy groups are essentially located on the silica support. It has been proposed that the surface vanadia species is basic towards alcohols, which are mildly acidic, and that is the reason for the preferential coordination of the surface methoxy species to the surface vanadia species rather

than the more acidic surface Si—OH site.⁶⁴ In line with this argument, the preferential coordination of the surface methoxy species to the silica support for supported niobium oxide and tungsten oxide system suggests that these surface metal oxides are more acidic than surface vanadia, which

agrees with the acidic character of these metal oxides. Furthermore, transient Raman studies have demonstrated that the surface Si—OCH₃ species are not reactive under the current methanol oxidation reaction conditions and are just spectator species.

For V₂O₅/TiO₂, The Ti—OCH₃ Raman bands decrease with increasing surface vanadia coverage and essentially disappear at monolayer coverage of surface vanadia species on titania,^{65,66} indicating that no V—OCH₃ species are detected in the V₂O₅/TiO₂ system by Raman spectroscopy. NbO_x/SiO₂ and WO_x/SiO₂ show the same trend.⁵⁹ The Zr—OMe Raman vibrations for vanadia/zirconia catalysts behave similarly to those of the V₂O₅/TiO₂ catalysts. No information was available for the V₂O₅/Al₂O₃ and Cr₂O₃/SiO₂ catalysts since the surface methoxy vibration region was obscured by fluorescence.^{36,37,59} However, complementary IR spectroscopic measurements demonstrated the existence of adsorbed V—OCH₃ species by the IR bands at ~2932 and ~2832 cm⁻¹.³⁶ Moreover, the surface vanadia monolayers of TiO₂, CeO₂, ZrO₂ and Al₂O₃ exhibit only V—OCH₃ bands and methanol appears to have no access to exposed support cation sites for the formation of support—OCH₃ species, consistent with the formation of a complete monolayer of surface vanadia on these oxide supports. In contrast, the 10% V₂O₅/SiO₂ catalyst contains both surface V—OCH₃ and Si—OCH₃ bands in the IR spectrum owing to the presence of exposed silica surface sites. Therefore, Raman spectroscopy presents some limitations for the

detection of surface methoxy species since it only detects surface methoxy bands on silica, V₂O₅/SiO₂, TiO₂ and ZrO₂ surfaces, with no V—OCH₃ bands being detected in the V₂O₅/TiO₂ or V₂O₅/ZrO₂ catalysts. This phenomenon is attributed to a support-induced effect upon the electronic structure of the surface V—OCH₃ species that reduces the Raman scattering cross-section in these catalysts. Consequently, *in situ* IR spectroscopy is a better method for the detection and quantification of chemisorbed surface methoxy intermediates on the active surface V₂O₅ sites during steady-state methanol oxidation and *in situ* Raman is a better method to study the molecular structural changes of the surface metal oxide species present in supported metal oxide catalysts.

The *in situ* Raman spectra during methanol oxidation over a 20% MoO₃/Al₂O₃ catalyst is shown in Fig. 7(A). Prior to methanol oxidation, the dehydrated and fully oxidized surface molybdenum oxide species, Mo(VI), gives rise to Raman bands at 1004, 862, 636 and 520 cm⁻¹, which are characteristic of polymeric surface molybdenum oxide species.⁶³ Exposure of this catalyst to methanol oxidation reaction conditions significantly reduces the terminal Mo=O bond vibration near 998 cm⁻¹ and creates new strong Raman bands at 840, 491 and 274 cm⁻¹, which are due to the reduced surface Mo(IV) species. Reoxidation of the reduced 20% MoO₃/Al₂O₃ catalyst significantly decreases the Raman vibrations associated with the reduced surface Mo(IV) species and increases the Raman bands associated with the surface Mo(VI) species. An analogous series of *in*

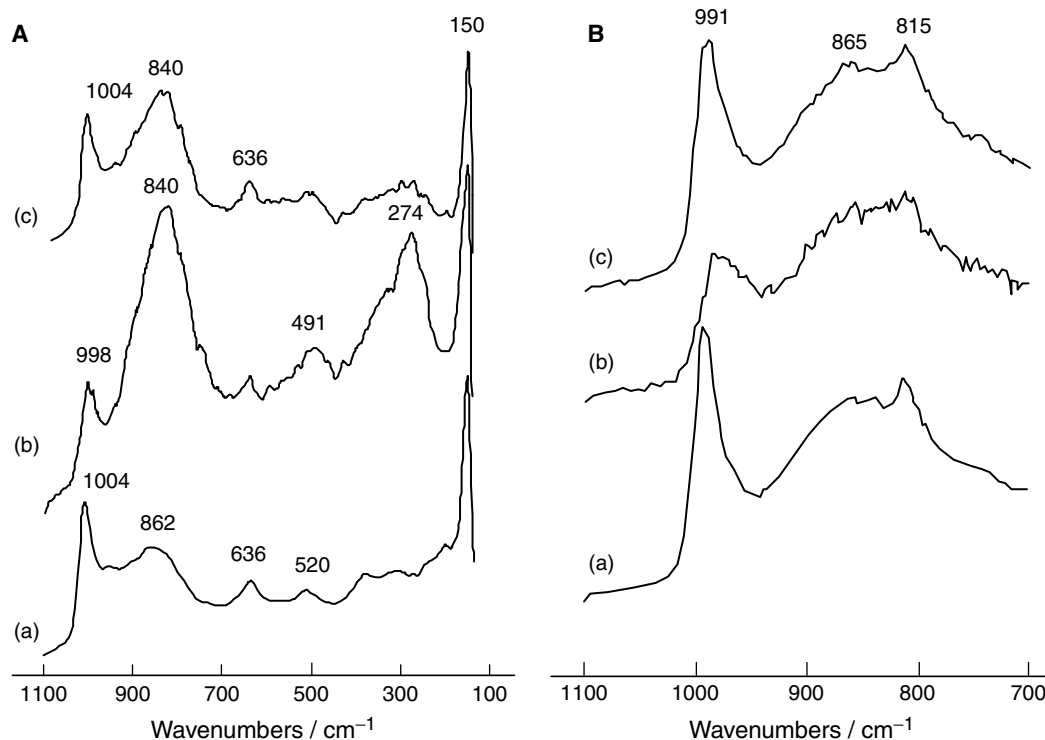


Figure 7. Reaction *in situ* Raman spectra of Mo(IV) species during methanol oxidation on 20% MoO₃/Al₂O₃ (A) and on 4% MoO₃/ZrO₂ (B). (a) dehydrated (b) during methanol oxidation at 503 K and (c) reoxidized dehydrated.

in situ studies over 4% MoO₃/ZrO₂ did not show Raman bands characteristic of reduced surface molybdenum oxide species [Fig. 7(B)].⁶³ For ZrO₂- and TiO₂-supported Cr₂O₃ catalysts, the surface chromate Raman signals disappear upon introducing a reducing CH₃OH/He gas feed due to reduction of Cr(VI) to Cr(III). In the case of SiO₂- or Al₂O₃-supported surface Cr₂O₃ species, no Raman bands are observed under a reducing CH₃OH/He gas feed owing to fluorescence from reduced surface chromium oxide species [especially the Cr(III) sites that are known to cause fluorescence].³⁷

REDUCTION CONDITIONS

Exposure of supported metal oxides (V, Cr, Mo) to reducing environments or during oxidation reaction conditions may lead to the formation of reduced surface metal oxide species that may be directly monitored by *in situ* Raman spectroscopy. However, as shown above for methanol oxidation and reduction, it appears that it is generally difficult to obtain good Raman signals for reduced surface metal oxide species of supported metal oxide catalysts. In contrast, the oxide supports do not appear to be reduced during the reduction of surface vanadia species. While the average oxidation state of reduced surface vanadia species can be quantitatively determined by temperature-programmed reduction (TPR) and gravimetric measurement, more specific information about the distribution of oxidation states can be obtained with *in situ* UV-Vis DRS studies, which are also informative about the chemical environment of the surface metal oxide sites. However, molecular information on the structures of the reduced surface oxide

species is not readily available, but may be obtained by *in situ* XANES/EXAFS measurements (especially if only one oxidation state is present under specific conditions).

Reduction by C₂–C₄ alkanes

In situ Raman studies of supported chromium oxide species under reducing conditions show that the specific oxide support has a pronounced effect. Silica-supported chromia catalysts show reduction under *n*-butane oxidation that leads to fluorescence and no visible Raman features can be detected. Zirconia-supported chromia exhibits Raman bands at 1030 cm⁻¹, characteristic of the terminal Cr=O bond of isolated surface chromate species, and the bands at 1010 and 880 cm⁻¹, characteristic of the terminal Cr=O and bridging Cr—O—Cr bonds of the surface polychromate species. Under *n*-butane oxidation reaction conditions, surface chromium oxide species reduce. The relative intensity of the bands at 880 and 1010 cm⁻¹ exhibit a parallel decrease in intensity, whereas the 1030 cm⁻¹ Raman band intensity decreases independently and at a slower rate. It is evident that each surface chromate species possesses different reduction properties. Therefore, polymeric surface chromium oxide species reduce more readily than the isolated surface chromium oxide species.

The *in situ* temperature-programmed Raman (TP-Raman) studies follow the evolution of a sample under controlled atmosphere vs temperature. The sample is heated stepwise and Raman spectra are recorded at each temperature. The *in situ* TP-Raman spectra of 1%V₂O₅/CeO₂ (Fig. 8) show Raman bands at 1017 and 860 cm⁻¹ that correspond to the polymeric surface vanadia species and a band at

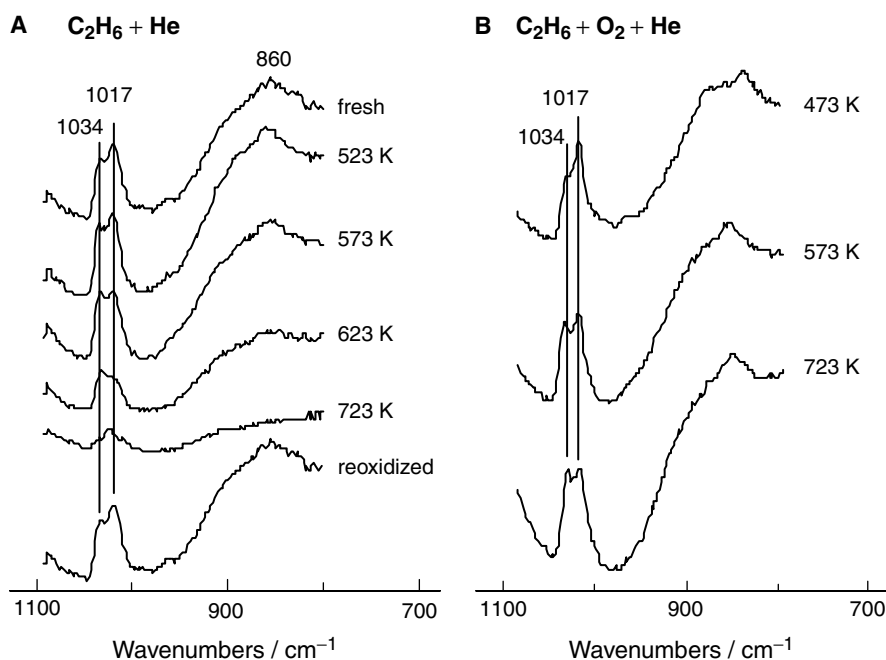


Figure 8. Reaction *in situ* (operando) Raman spectroscopy of 1%V₂O₅/CeO₂ under C₂H₆/He (A) and C₂H₆/O₂/He (B) reaction feed.

1034 cm^{-1} corresponding to isolated surface vanadia sites. Under a reducing atmosphere ($\text{C}_2\text{H}_6 + \text{He}$), the polymeric surface vanadia species are more easily reduced than the isolated surface vanadium sites, as reflected by the preferential decrease of the two Raman bands characteristic of polymeric surface vanadia species during the TP-Raman experiment [Fig. 8(A)]. Under reaction conditions ($\text{C}_2\text{H}_6 + \text{O}_2 + \text{He}$), however, only a small fraction of the surface vanadia sites were reduced since at 723 K the Raman spectrum remains very similar to the Raman spectrum of the fresh, dehydrated sample [Fig. 8(B)]. *In situ* UV-Vis DRS spectroscopy measures no significant reduction for the silica- and alumina-supported vanadia catalysts during ethane oxidation.⁴⁷ The 1% $\text{V}_2\text{O}_5/\text{ZrO}_2$ catalyst shows a slight vanadia reduction during ethane oxidation and only 5.5% reduction is observed during ethane reduction. Thus, the average oxidation state under steady-state oxidation conditions does not rely on the reducibility of the catalyst, but on the equilibrium of the reduction and reoxidation rates of the catalytic cycle. UV-Vis DRS spectroscopy is also sensitive to the degree of polymerization of surface vanadia species.⁵⁰ During ethane oxidation, the edge energy values are essentially unchanged on silica- or alumina-supported vanadia, but increase on more reducible supports like zirconia, which indicates preferential reduction of the surface polymerized species. The polymerization degree of the surface V(V) cations increases from the 1% to 4% $\text{V}_2\text{O}_5/\text{ZrO}_2$ catalysts owing to the higher surface vanadia density.⁴⁷ The polymerized surface vanadia species on 4% $\text{V}_2\text{O}_5/\text{ZrO}_2$ are more easily reduced than the 1% $\text{V}_2\text{O}_5/\text{ZrO}_2$ under ethane reduction conditions at 723 K (23.0% vs 5.5% reduction). The *in situ* TP-Raman spectra of 1% $\text{V}_2\text{O}_5/\text{CeO}_2$ provide further evidence for the preferential reduction of polymeric surface vanadia species over the isolated surface vanadia species.

The extent of reduction of supported metal oxide catalysts is dependent on the hydrocarbon reactivity. *In situ* temperature-programmed reduction Raman (TPR-Raman) studies consist of a stepwise temperature-programmed reduction and Raman spectra are acquired at every step. *In situ* TPR-Raman experiments with 17.5% $\text{V}_2\text{O}_5/\text{Al}_2\text{O}_3$ under reducing $\text{C}_4\text{H}_{10}/\text{He}$ feed shows the complete disappearance of the Raman bands of the surface vanadium oxide species at 623 K.⁴⁵ However, 15% $\text{V}_2\text{O}_5/\text{Al}_2\text{O}_3$ under a reducing $\text{C}_2\text{H}_6/\text{He}$ gas feed shows a very strong decrease in the Raman bands at 803 K, but not complete reduction.⁴⁷ However, it is important to stress that even when surface polymeric metal oxide species are more reducible than the isolated surface metal oxide species, there is not much difference between the extent of reduction of surface metal oxide monomers and polymers during steady-state hydrocarbon oxidation reactions. The average oxidation state during catalytic operation depends on the balance between the reduction by the hydrocarbon molecule and the reoxidation by gas-phase molecular oxygen, and it does appear that reoxidation is faster than reduction. Therefore, supported

metal oxide catalysts are essentially oxidized during catalytic operation and exhibit a zero-order dependence on the oxygen partial pressure. Furthermore, oxygen isotopic switching experiments⁶⁷ and comparative temperature-programmed reaction spectroscopy (TPRS) experiments with and without oxygen⁴⁸ demonstrate that the surface lattice oxygen, and not gas-phase oxygen, is involved in these oxidation reactions via a Mars-van Krevelen mechanism.

Reduction in hydrogen and reoxidation

In general, it appears that supported vanadia and chromia catalysts show no new Raman bands for their reduced surface metal oxide species.^{58,68} However, the structural changes taking place upon reduction of supported metal oxides may influence the structure of the reoxidized metal oxide phase. Thus, *in situ* TPR-Raman studies⁶⁹ demonstrate the dynamic states of silica-supported vanadium oxide species. During the TPR of 0.9% $\text{V}_2\text{O}_5/\text{SiO}_2$ (~30% of maximum surface coverage for this specific silica), the Raman intensity of the terminal $\text{V}=\text{O}$ bond of the surface vanadium oxide species at 1037 cm^{-1} decreases monotonically with H_2 consumption during the experiments. Upon reoxidation, the 0.9% $\text{V}_2\text{O}_5/\text{SiO}_2$ catalyst exhibits only the Raman band of the original surface vanadia species.⁶⁹ However, a sample with 2.4% $\text{V}_2\text{O}_5/\text{SiO}_2$, close to the maximum coverage of surface vanadium oxide for this specific silica, undergoes structural modification upon hydrogen reduction and reoxidation (Fig. 9). At 473 K, during H_2 -TPR, new Raman bands at 994, 702, 284 and 146 cm^{-1} appear which are characteristic of crystalline V_2O_5 . As the temperature increases during the TPR, the Raman bands of crystalline V_2O_5 become more evident and then completely disappear owing to reduction of V_2O_5 to V_2O_3 (black phase with extremely low Raman scattering signal). The Raman band of the isolated surface vanadium oxide species at 1037 cm^{-1} persists up to 823 K, which reflects its stability as surface V(V) species. The TPO (Temperature Programmed Oxidation)-Raman spectra demonstrate the formation of both crystalline V_2O_5 and isolated surface vanadium oxide species. Therefore, near the maximum surface coverage, the $\text{V}_2\text{O}_5/\text{SiO}_2$ catalyst does not completely undergo a reversible change modification during the redox cycles. Under reducing conditions, the surface vanadium oxide species reduce and produce no new Raman signal, and therefore no information is available about the reduced surface vanadium oxide species [quantitative H_2 consumption demonstrate that it is reduced to surface V(III) species]. However, as the surface vanadia coverage increases, it is more likely to compensate for O removal by sharing oxygen sites among the surface vanadium oxide species. Raman, XANES and ^{51}V -NMR studies⁷⁰ show that surface vanadia on silica may exist in two extreme configurations under dehydrated conditions, isolated surface vanadia species and crystalline V_2O_5 , but not as polymeric surface vanadia species. Thus, any effect that promotes interaction among surface vanadia species must lead to

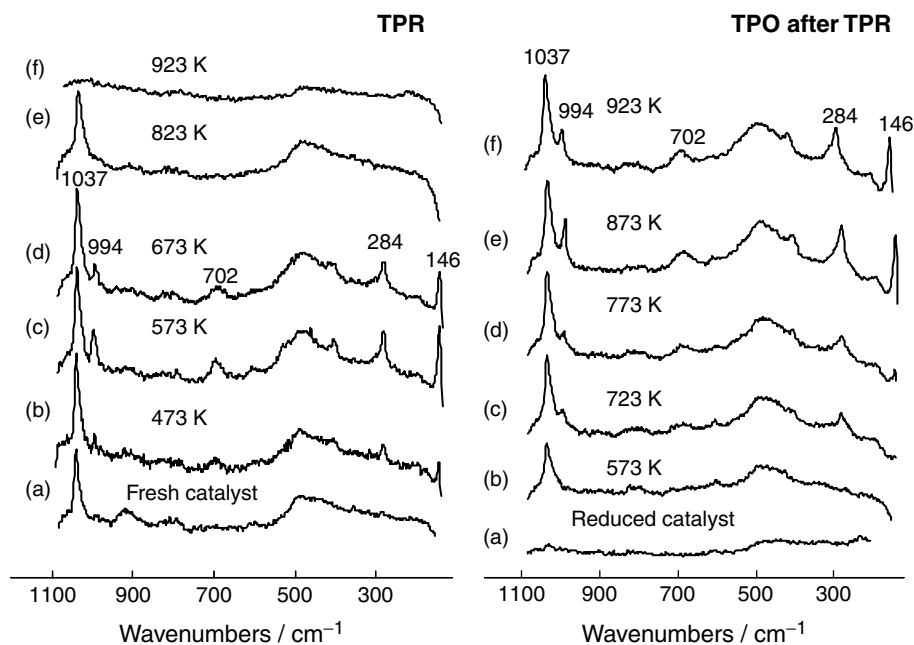


Figure 9. Selected Raman spectra of V_2O_5/SiO_2 during TPR-Raman spectroscopy of fresh sample (left) and during TPO-Raman spectroscopy of the reduced sample (right).

the formation of crystalline V_2O_5 , as reflected by the TPR-Raman experiments.⁶⁹ However, the Raman signal of V_2O_5 crystals is about 10 times more intense than that of surface VO_x species.⁷¹ Hence only a very minor portion of the surface VO_x species aggregates to microcrystals during reduction/oxidation cycles.

STRUCTURAL TRANSFORMATIONS UNDER DIFFERENT ENVIRONMENTS

Under dry air

While supported metal oxides are stable under dehydrated conditions, an increase in temperature may sometimes lead to structural transformation of the surface metal oxide species through solid-state reaction with the underlying oxide support. The intrinsic thermal stability of 12-molybdophosphoric acid ($H_3PMo_{12}O_{40}$), HPMo, can be altered by depositing it on an oxide support. Bulk HPMo decomposes at 673 K into β - MoO_3 , as shown by Raman bands at 851 and 775 cm^{-1} .⁷² At 773 K, the α - and β - MoO_3 phases co-exist and α - MoO_3 dominates at 823 K.⁷² On heating silica-supported HPMo, a progressive degradation of the HPMo phase is evident and at 823 K the Raman bands at 993, 861, 818 and 280 cm^{-1} reveal that a mixture of α - and β - MoO_3 co-exist [Fig. 10(A–f)]. The presence of α - MoO_3 at 923 K is evident from the Raman bands at 990, 816, 657, 333 and 282 cm^{-1} [Fig. 10(A–g)]. HPMo supported on ZrO_2/SiO_2 decomposes at lower temperatures than bulk HPMo and new Raman bands start to form at 990, 970, 770 and 360 cm^{-1} . The Raman band at 990 cm^{-1} is sensitive to hydration/dehydration, and corresponds to surface molybdenum oxide species. The Raman

bands at 970, 770 and 360 cm^{-1} are not affected by hydration/dehydration and correspond to $Zr(MoO_4)_2$. The formation of the $Zr(MoO_4)_2$ phase is promoted by temperature and the zirconia content.⁷²

In situ TP-Raman in dry air of ZrO_2 -supported Sb–V metal oxides exhibits that both Zr and Sb react with the V species.⁷³ The interaction between Sb and V depends on the total Sb + V surface coverage on zirconia. The interaction of the surface vanadium oxide species with zirconia support in the absence of Sb leads to the formation of ZrV_2O_7 at elevated temperatures. This process is easier on zirconium hydroxide and does not require the presence of crystalline V_2O_5 .⁷³ $SbVO_4$ phases form at surface coverage near or beyond a monolayer on zirconia. The interaction of surface vanadia species with Sb suppresses the formation of ZrV_2O_7 .

Under humid air

In other supported metal oxides, prolonged exposure to moisture may further lead to important structural changes due to the amount of water present on the catalyst. Bañares, Hu and Wachs⁶¹ used *in situ* Raman spectroscopy to investigate a 5% MoO_3/SiO_2 catalyst under flowing oxygen saturated with water vapor at different temperatures to follow the structural changes of the surface molybdenum oxide species (Fig. 11). The silica support exhibits Raman bands at 800, 602 and 485 cm^{-1} . The intense Raman band at 980 cm^{-1} corresponds to the stretching mode of the terminal $Mo=O$ bond of the dehydrated monomeric surface molybdenum oxide species on silica. The surface Mo oxide Raman band overwhelms the weaker band of silica Si–OH vibrations at ~ 970 cm^{-1} . A weaker Raman

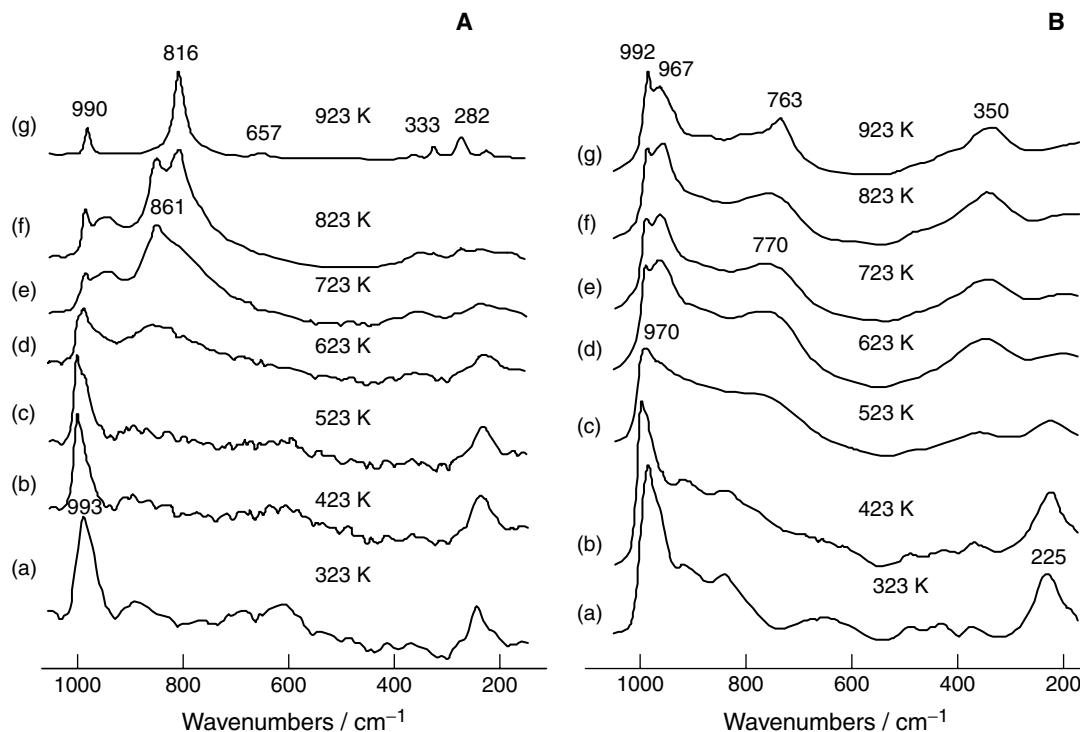


Figure 10. Representative *in situ* TP-Raman spectra of HPMo/SiO₂ (A) and HPMo/9.6%ZrO₂/SiO₂ (B) at different temperatures in dry air.

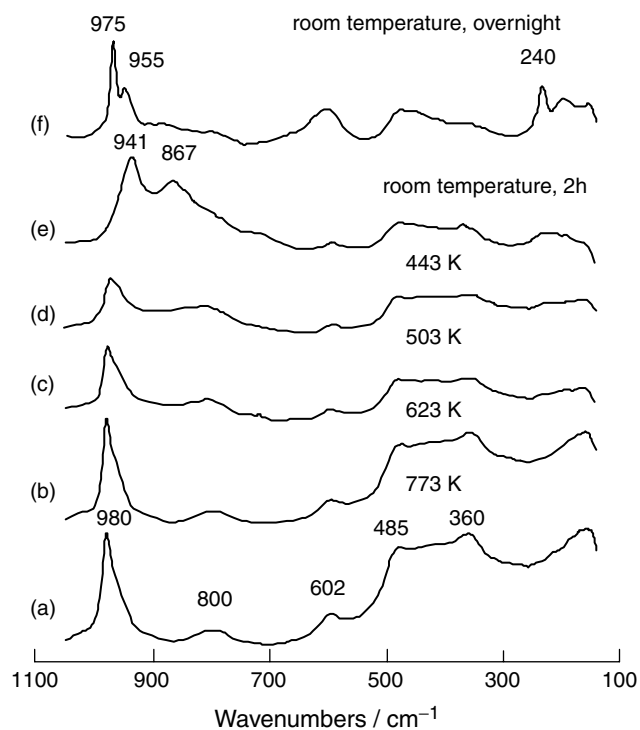


Figure 11. *In situ* Raman spectra of 5% MoO₃/SiO₂ catalysts in flowing air saturated with water as a function of decreasing temperature.

band $\sim 360\text{ cm}^{-1}$ corresponds to the bending mode of the surface molybdate species [Fig. 11(a)]. No significant changes can be observed on decreasing the temperature from 773 to 503 K [Fig. 11(a)–(c)], which suggests that the catalyst remains in a dehydrated state at these temperatures under the flow of water vapor. At room temperature, Raman bands that are characteristic of heptamolybdate (Mo₇O₂₄⁶⁻) (944, 867, 370 and 240 cm⁻¹) species appear after 2 h [Fig. 11(e)]. Further changes are observed in the Raman spectrum of MoO₃/SiO₂ upon overnight exposure to the hydrated stream at room temperature: new Raman bands are observed at 975, 955, 614 and 240 cm⁻¹, which correspond in position and relative intensity to β -silicomolybdic acid (H₄SiMo₁₂O₄₀)⁷⁴ [Fig. 11(f)]. This shows a partial dissolution of the oxide support due to a large amount of adsorbed water since ca 50% of the sample weight is water.⁶¹ The solubilization of the support under extreme moisture conditions has also been observed more recently by Carrier *et al.*⁷⁵ and Le Bihan *et al.*⁷⁶ for alumina-supported molybdenum oxide species. However, these hydrated metal oxide complexes tend to decompose at elevated temperatures owing to the loss of moisture.

The presence of moisture may also lead to extensive transformations of supported metal oxides. Such is the case for silica-supported molybdenum oxide. Under ambient conditions, the structure of surface molybdenum oxide species is a hydrated surface polymolybdate species (Mo₇O₂₄⁶⁻) whose structure depends on the surface pH at point of zero

charge (PZC) of the catalyst, as discussed elsewhere (see above). The formation of silicomolybdic acid ($\text{H}_4\text{SiMo}_{12}\text{O}_{40}$), SMA, has also been reported upon exposure to significant moisture at room temperature.^{77–79} The SMA is a Keggin-type structure consisting of 12 octahedral MoO_6 surrounding a SiO_4 tetrahedron.⁸⁰ Cohesion between the Keggin units is achieved by means of hydrated protons and water molecules.⁸¹ Upon dehydration, the polymolybdate structures are unstable and spread over the silica surface to form isolated surface molybdenum oxide species.⁸²

The effect of heating silica-supported SMA in an $\text{H}_2\text{O}/\text{O}_2$ feed is presented in the Raman spectra in Fig. 12.⁶¹ At room temperature, it exhibits the Raman bands of SMA (975, 955, 614 and 241 cm^{-1}) and a weak band at $\sim 818\text{ cm}^{-1}$, due to traces of $\alpha\text{-MoO}_3$. At 473 K, Raman features are observed near 996 and 240 cm^{-1} as well as a shoulder at $\sim 977\text{ cm}^{-1}$ [Fig. 12(b)]. The 996, 977 and 240 cm^{-1} bands are assigned to dehydrated surface $\beta\text{-SMA}$ species and the shift of the 975 cm^{-1} Raman band to higher wavenumber is consistent with shortening of the terminal $\text{Mo}=\text{O}$ bond upon dehydration. The presence of the Raman band at $\sim 240\text{ cm}^{-1}$ (characteristic of $\text{Mo}-\text{O}-\text{Mo}$ vibrations) also reveals that the $\beta\text{-SMA}$ species is still present on the silica surface. Similar features are also present at 503 K [Fig. 12(c)]. The Raman spectrum at 573 K shows that the Raman band at $\sim 996\text{ cm}^{-1}$ has disappeared and that the band at ca 240 cm^{-1} has broadened considerably [Fig. 12(d)].

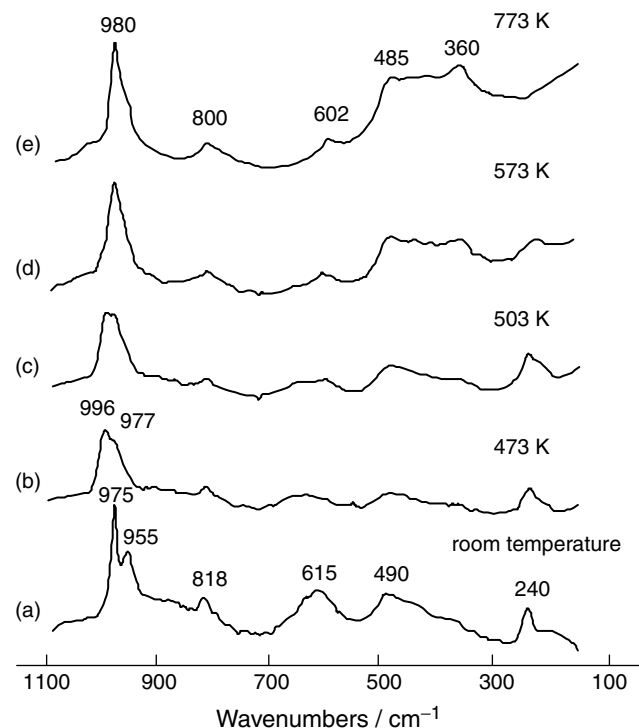


Figure 12. *In situ* Raman spectra of 5% MoO_3 (as SMA) on silica in flowing oxygen saturated with water as a function of increasing temperature.

The Raman spectrum at 773 K exhibits a band at 980 cm^{-1} that is characteristic of the terminal $\text{Mo}=\text{O}$ bond of isolated surface molybdenum oxide species on silica and no band at $\sim 240\text{ cm}^{-1}$, which is characteristic of bridging $\text{Mo}-\text{O}-\text{Mo}$ vibrations [Fig. 12(e)]. In the absence of moisture, the trends are identical with those observed in the $\text{H}_2\text{O}/\text{O}_2$ stream.⁶¹ Thus, silica-supported SMA species are not stable at 573 K regardless of the presence or absence of moisture. Hence the catalytic performance of $\text{MoO}_3/\text{SiO}_2$ and SMA/SiO_2 catalysts with the same loading of molybdenum oxide should be identical for reactions operating at temperatures higher than 573 K. This has been shown for the selective oxidation of methane.⁶¹ Both catalysts show the same activity, formation of formaldehyde, CO and CO_2 , and the selectivity–conversion profiles for each product are identical for both catalysts.⁶¹

Under ethane oxidation reaction conditions

The *in situ* Raman spectra of dehydrated supported VO_x/CeO_2 catalysts demonstrate the disappearance of the band for the surface vanadia species with increasing temperature, which is accompanied by the formation of new intense Raman bands that are characteristic of the bulk CeVO_4 phase ($840, 774, 768, 458, 369, 259, 215$ and 146 cm^{-1}).⁴⁷ It is also interesting to underline that the selectivity trends for the VO_x/CeO_2 series after the solid-state reaction approaches that of pure CeVO_4 (M. A. Bañares, M. V. Martínez-Huerta, X. Gao, J. L. G. Fierro and I. E. Wachs, presented at the 220th ACS Symposium, Washington, DC, 2000). A detailed *in situ* Raman spectroscopic investigation under ethane oxidation reaction conditions with on-line activity measurement (operando Raman spectroscopy) was performed for the VO_x/CeO_2 system (M. A. Bañares, M. V. Martínez-Huerta, X. Gao, J. L. G. Fierro and I. E. Wachs, presented at the 220th ACS Symposium, Washington, DC, 2000). It was found that disappearance of the surface vanadium oxide species with simultaneous formation of the bulk CeVO_4 phase does not alter the catalytic activity, as evidenced by simultaneous on-line GC analyses during operando Raman spectroscopy. When the reaction temperature increases, the crystallinity of the bulk CeVO_4 phase increases and ethane conversion decreases. The crystal quality of CeVO_4 phase was estimated according to the FWHM of its Raman bands. The activation energy does not change because of the structural transformation from surface VO_x species on CeO_2 to $\text{CeVO}_4/\text{CeO}_2$. Therefore, it appears that it is not the nature of the active site that changes, but only the number of active surface sites decreases. Hence the nature of the active surface site does not change upon formation of CeVO_4 from surface VO_x species on ceria (M. A. Bañares, M. V. Martínez-Huerta, X. Gao, J. L. G. Fierro and I. E. Wachs, presented at the 220th ACS Symposium, Washington, DC, 2000). Therefore, incipient formation of CeVO_4 does not significantly decrease the number of available surface VO_x sites, while an increase in the crystallization of the bulk CeVO_4 phase results in a

lower number of available surface VO_x sites, thus decreasing total activity. This conclusion would not have been available through just *in situ* Raman studies, which underlines the advantage of the additional information provided by operando Raman studies.

Under methanol oxidation reaction conditions

The *in situ* Raman spectrum of 5% $\text{MoO}_3/\text{SiO}_2$ during methanol oxidation reveals the presence of adsorbed surface methoxy groups at 2995 and 2957 and 2857 cm^{-1} , assigned to $\text{Si}-\text{OCH}_3$. Increasing the surface molybdenum oxide coverage decreases the Raman intensities of these bands owing to titration of the $\text{Si}-\text{OH}$ sites by the deposited Mo oxide, which demonstrates that the molybdenum oxide is well dispersed on the silica support. The dispersed and isolated surface molybdenum oxide species ($\sim 980\text{ cm}^{-1}$) transforms into microcrystalline $\beta\text{-MoO}_3$ (Raman bands at 842 and 768 cm^{-1}) during methanol oxidation at 503 K .^{59,62} At very low surface molybdenum oxide coverage, this aggregation is hardly appreciable, probably owing to the low probability of interaction among the surface molybdenum oxide species. However, the formation of the microcrystalline $\beta\text{-MoO}_3$ phase becomes more intense with increasing surface molybdenum oxide loading, at $\sim 5\%$ $\text{MoO}_3/\text{SiO}_2$ [Fig. 13(A)]. This is the reason for the progressive decrease in the apparent TOF values for methanol oxidation with surface molybdenum oxide coverage on silica.⁶² The decrease in methanol conversion with surface molybdenum oxide coverage is mainly due to this sintering phenomenon and results in a significant decrease in the methyl formate

formation while HCHO production shows a smoother decrease with surface molybdenum oxide loading. These trends depend only on the surface molybdenum oxide coverage and are essentially independent of preparation method and the specific silica support. There are two surface sites for methanol oxidation over silica-supported catalysts: surface molybdenum oxide sites and silanol groups. Surface molybdenum oxide sites that interact with methanol form HCHO that may desorb or further interact with nearby surface $\text{Si}-\text{OCH}_3$ to form dimer product of methyl formate. The increase in surface molybdenum oxide coverage has a negative effect on the formation of methyl formate since the surface molybdenum oxide species rearranges to crystalline $\beta\text{-MoO}_3$, which almost exclusively forms H_2CO . These structural effects account for the significant decrease in methanol conversion to methyl formate that requires both adjacent surface molybdenum oxide species and exposed surface silanol sites.⁶²

The *in situ* Raman spectra of 5% $\text{Re}_2\text{O}_7/\text{SiO}_2$ under methanol oxidation reactions conditions exhibit the vibrations of surface $\text{Si}-\text{OCH}_3$ (Raman bands at 2956 and 2856 cm^{-1}).⁵⁹ The catalyst also exhibits Raman bands at 1010 , 973 and 340 cm^{-1} [Fig. 13(B)], characteristic of surface rhenium oxide species,³⁵ in addition to the Raman bands at 800 , 601 and 485 cm^{-1} due to the silica support. The silica support also has an $\text{Si}-\text{OH}$ Raman vibrational mode at $\sim 973\text{ cm}^{-1}$, but its intensity is much weaker than the Raman band at $\sim 973\text{ cm}^{-1}$ of the surface Re oxide species. Under reaction conditions, the surface rhenium oxide species become volatile, as reflected by the absence of Raman features of

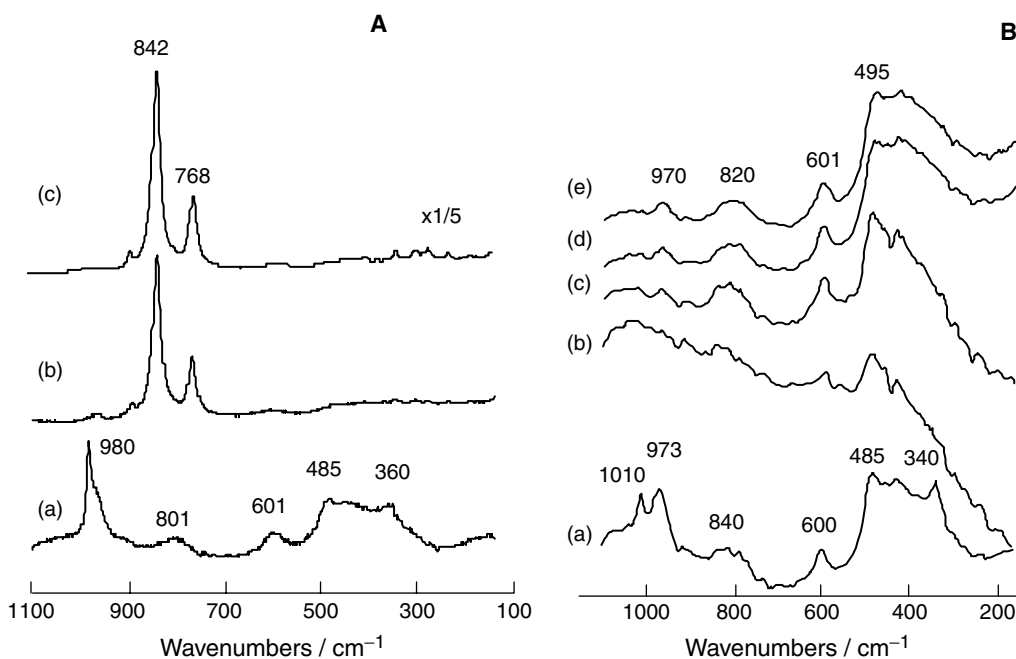


Figure 13. (A) Reaction *in situ* (operando) Raman spectra of 5% $\text{MoO}_3/\text{SiO}_2$; (B) 5% $\text{Re}_2\text{O}_7/\text{SiO}_2$ catalysts at various stages of methanol oxidation reaction. (a) O_2 , 503 K ; (b) $\text{CH}_3\text{OH}/\text{O}_2/\text{He}$, 503 K ; (c) O_2/He , 503 K ; (d) O_2 , 573 K ; (e) O_2 , 623 K .

the surface rhenium oxide species after reoxidation of the samples [Fig. 13(B-c)].⁵⁹

The mobility and volatility of surface Mo and Re oxides are enhanced by the formation of metal oxide–methoxy complexes. The Raman bands for the terminal M=O bonds decrease in intensity and shift to lower wavenumbers during methanol oxidation.^{35,59} The mobility of the surface molybdenum oxide and the volatility of the rhenium oxide species on the silica support are attributed to the formation of M—OCH₃ complexes. These complexes result in the volatilization of the surface rhenium oxide species and the crystallization of the surface molybdenum oxide species. The Mo—OCH₃ species were also somewhat volatile because Mo deposits were detected on the glass portion of the reactor exit.⁶² The strong interaction of surface molybdenum oxide species with methanol that leads to its structural rearrangement into microcrystalline β -MoO₃ also affects the stability of silica-supported silicomolybdic acid, which at 573 K under methanol oxidation reaction conditions forms β -MoO₃.⁶¹

CONCLUSIONS

Raman spectroscopy is a very versatile molecular characterization technique for studying supported metal oxide catalysts under different environments. Dehydrated supported metal oxide species consist of metal cations surrounded by oxygen ions, one of which is a terminal M=O bond and the others bridge the cations to the oxide support (M—O—support) or to adjacent surface cations (M—O—M). Exposure to moisture leads to coordination of water, which under reaction conditions may compete with reacting molecules. At high temperature, moisture readily exchanges oxygens in the supported metal oxides. The interaction with moisture becomes more pronounced as the temperature decreases. At ambient temperature, this interaction leads to the solvation and even the dissolution of the supported oxides. Under ambient conditions, the molecular structures of the hydrated supported metal oxides are determined by their chemistry in aqueous solutions, which depends on their concentration and solution pH. The pH value corresponds to the PZC (point of zero charge). The pH at PZC value is determined by (1) the specific oxide support, (2) the specific active supported metal oxide and (3) the surface coverage of the active supported metal oxide. The presence of extensive water may also lead to a partial dissolution of the oxide support cation.^{61,75,76}

Dehydrated polymeric surface metal oxide species are preferentially reduced over the corresponding dehydrated surface monomeric species. Under reaction conditions, however, the average oxidation state does not depend on the reducibility of the surface oxide but on the balance between reduction and reoxidation rates during the catalytic process. The catalytic reactivity of the supported metal oxide catalysts does not appear to be associated with the terminal

M=O bond, which is too stable to be directly involved in the kinetically critical rate-determining step. The bridging oxygen sites among surface metal oxide cations, M—O—M, do not appear to have a significant role since the TOF values are not affected by the coverage of the active surface metal oxide species. Several independent factors strongly suggest that the V—O—support bridging oxygen is the kinetically critical active site during oxidation reactions since changing the oxide support ligand can influence the TOF values by orders of magnitude. In some cases, as in the oxidation of *n*-butane to maleic anhydride, surface coverage does have a strong effect and the TOF values increase, but this is related to a geometric requirement of several sites in close vicinity for an efficient activation of the *n*-butane molecule and its oxidation by four oxygen atoms to yield maleic anhydride. Similarly, the bimolecular reaction between NO_x and NH₃ during SCR requires two adjacent surface acid and redox sites and the TOF value increases with surface metal oxide coverage. However, for unimolecular oxidation reactions that require only the consumption of one surface oxygen atom, only one surface active metal oxide site appears to be required (methanol to formaldehyde,^{59,60,63} methane to formaldehyde,^{53,54} ethane to ethylene,^{20,38,47} propane to propylene,^{48,49} 1-butene to butadiene⁸³ and SO₂ to SO₃⁸⁴).

A complete fundamental understanding of the structural changes of supported metal oxides under different environments cannot always be fully understood just through *in situ* Raman spectroscopy, but requires the application of complementary spectroscopic characterization techniques. Also, the incorporation of simultaneous catalytic activity and selectivity measurement with the spectroscopic studies under reaction conditions (operando spectroscopy) provides key information to be able to understand more fully the structure–activity/selectivity relationship at a molecular level for supported metal oxide catalysts.

The performance of bulk mixed-metal oxides must be determined by the nature of the outermost surface layer, directly exposed to reacting molecules rather than by the bulk structure. Recent studies have revealed that the surfaces of bulk mixed molybdates are covered by monolayers of surface Mo oxide.^{85,86} Therefore, we are now at the dawn of a new approach to understanding fundamentally the molecular structure–activity/selectivity relationship of bulk mixed-metal oxide catalysts, since the knowledge developed for supported metal oxides in the past decade can be directly applied to the molecular-level understanding of bulk mixed-metal oxide catalysts.

Acknowledgements

The financial support of the US National Science Foundation (NSF), grant CTS-9901643, US Department of Energy (DOE), Basic Energy Sciences, grant DE-FG02-93ER14350, and CICYT, Spain (Projects QUI98-0784 and IN96-0053) for this collective work is greatly appreciated.

The authors also thank all the individuals in their laboratories at Lehigh University and the Institute of Catalysis and Petroleum

Chemistry who have made significant contributions to the advancement of Raman spectroscopy of catalysis; without their contributions we would not possess all the fundamental knowledge that we have today: Frank D. Hardcastle, Jih-Mirm Jehng, Goutam Deo, Dou-soung Kim, Michael A. Vuurman, Andrzej M. Turek, Hangchun Hu, Xingtao Gao, Bert Weckhuysen, Vadim Gulians, Loyd Burcham, Chuan-Bao Wang, Yeping Cai, M. Victoria Martínez-Huerta and M. Olga Guerrero-Pérez.

REFERENCES

- Thomas JM, Thomas WJ. *Principles and Practice of Heterogeneous Catalysis*. VCH: New York, 1997.
- Wachs IE. In *Handbook of Spectroscopy*, Lewis IR, Edwards HGM (eds). Marcel Dekker: New York, 2001; chapt. 20, 799–833.
- Bartlett JR, Cooney RP. In *Spectroscopy of Inorganic-Based Materials*, Clark RJH, Hester RE (eds). Wiley: New York, 1987; 187.
- Stencel JM. *Raman Spectroscopy for Catalysis*. Van Nostrand: New York, 1990.
- Mehicic M, Grasselli JG. In *Analytical Raman Spectroscopy*, Grasselli JG, Bulkin BJ (eds). Wiley: New York, 1991.
- Wachs IE, Hardcastle FD. In *Catalysis—A Specialist Periodical Report*, vol. 10, Royal Society of Chemistry: Cambridge, 1993; 102.
- Wachs IE. *Catal. Today* 1996; **27**: 437.
- Wachs IE. *Top. Catal.* 1999; **8**: 57.
- J. Raman Spectrosc.* 2002; **33**: Special Issue.
- Wachs IE. In *Raman Scattering in Materials Science*, Weber WH, Merlin R (eds). Springer: Berlin, 2000; 271.
- Wachs IE, Segawa K. In *Characterization of Catalytic Materials*, Wachs IE (ed.). Butterworths: Stoneham, MA, 1992; 69–88.
- Mestl G, Srinivasan TKK. *Catal. Rev. Sci. Eng.* 1998; **40**: 451.
- Mestl G. *J. Mol. Catal. A* 2000; **158**: 45.
- Knözinger H, Mestl G. *Top. Catal.* 1999; **8**: 45.
- Payen E, Kasztelan S. *Trends Phys. Chem.* 1994; **4**: 363.
- Weckhuysen BM. *Chem. Commun.* 2000; 97.
- Weber WH. *Mater. Sci.* 2000; **42**: 233.
- Thomas CL. *Catalytic Processes and Proven Catalysts*. Academic Press: New York, 1970.
- Centi G, Trifirò F. *New Developments in Selective Oxidation*. Elsevier: Amsterdam, 1994.
- Bañares MA, Gao X, Fierro JLG, Wachs IE. *Stud. Surf. Sci. Catal.* 1997; **107**: 295.
- Wachs IE. *US Patent* 5907066, 1999; Wachs IE. *US Patent* 6084135, 2000; Wachs IE. *US Patent* 6198005, 2001.
- Gao X, Bare SR, Weckhuysen BM, Wachs IE. *J. Phys. Chem. B* 1998; **102**: 10842.
- Gao X, Wachs IE. *J. Catal.* 2000; **192**: 18.
- Gao X, Bare SR, Fierro JLG, Wachs IE. *J. Phys. Chem. B* 1999; **103**: 618.
- Gao X, Fierro JLG, Wachs IE. *Langmuir* 1999; **15**: 3169.
- Williams CC, Ekerdt JG, Jehng J-M, Hardcastle FD, Turek AM, Wachs IE. *J. Phys. Chem.* 1991; **85**: 8781.
- Hu H, Wachs IE, Bare SR. *J. Phys. Chem.* 1995; **99**: 10897.
- Williams CC, Ekerdt JG, Jehng J-M, Hardcastle FD, Wachs IE. *J. Phys. Chem.* 1991; **95**: 8791.
- Deo G, Wachs IE. *J. Phys. Chem.* 1991; **95**: 5889.
- Gil-Llambias FJ, Escudéy AM, Fierro JLG, Agudo AL. *J. Catal.* 1985; **95**: 520.
- Linschke G, Hanke W, Jerschke HG, Oehlmann G. *J. Catal.* 1985; **91**: 54.
- Tanaka T, Yamashita H, Tsuchitani R, Funabiki T, Yoshida S. *J. Chem. Soc., Faraday Trans. 1* 1988; **84**: 2987.
- Nakamoto K. *Infrared and Raman Spectra of Inorganic and Coordination Compounds* (5th edn). Wiley: New York, 1997.
- Banwell CN. *Fundamentals of Molecular Spectroscopy* (3rd edn). McGraw-Hill: London, 1983.
- Weckhuysen BM, Jehng J-M, Wachs IE. *J. Phys. Chem. B* 2000; **104**: 7382.
- Burcham LJ, Deo G, Gao X, Wachs IE. *Top. Catal.* 2000; **11/12**: 85.
- Weckhuysen BM, Wachs IE. *J. Phys. Chem. B* 1996; **100**: 14437.
- Bañares MA, Martínez-Huerta M, Gao X, Wachs IE, Fierro JLG. *Studs. Surf. Sci. Catal.* 2000; **130**: 3125.
- Bañares MA, Martínez-Huerta MV, Wachs IE. *4th World Congress on Oxidation Catalysis, Book of Extended Abstracts*, vol. II. 2001; 315.
- Jehng J-M, Deo G, Weckhuysen BM, Wachs IE. *J. Mol. Catal. A* 1996; **110**: 41.
- Hardcastle FD, Wachs IE. *J. Phys. Chem.* 1991; **95**: 5031.
- Duffy BL, Curry-Hyde HE, Cant NW, Nelson PF. *J. Phys. Chem.* 1994; **98**: 7153.
- Topsøe NY, Sobalik T, Clausen BS, Srnak TZ, Dumesic JD. *J. Catal.* 1992; **134**: 742.
- Odenbrand LAH, Gabrielsson PLT, Brandin JGM, Andersson LAH. *Appl. Catal.* 1991; **78**: 109.
- Wachs IE, Jehng J-M, Deo G, Weckhuysen BM, Gulians V, Benziger JB. *Catal. Today* 1996; **32**: 47.
- Wachs IE, Jehng J-M, Deo G, Weckhuysen BM, Gulians VV, Benziger JB, Sundaresan S. *J. Catal.* 1997; **170**: 75.
- Bañares MA, Martínez-Huerta MV, Gao X, Fierro JLG, Wachs IE. *Catal. Today* 2000; **61**: 295.
- Gao X, Jehng J-M, Wachs IE. *J. Catal.* in press.
- Watling TC, Deo G, Seshan K, Wachs IE, Lercher JA. *Catal. Today* 1996; **28**: 139.
- Gao X, Bañares MA, Wachs IE. *J. Catal.* 1999; **188**: 325.
- Cardoso JH. *PhD Dissertation*, Universidade Federal de São Carlos, São Paulo, 1998.
- Datka J, Turek AM, Jehng J-M, Wachs IE. *J. Catal.* 1992; **135**: 186.
- Bañares MA, Spencer ND, Jones MD, Wachs IE. *J. Catal.* 1994; **146**: 204.
- Sun Q, Jehng J-M, Hu H, Herman RG, Wachs IE, Klier K. *J. Catal.* 1997; **165**: 101.
- Bielanski A, Haber J. *Catal. Rev. Sci. Eng.* 1979; **19**: 1.
- Wachs IE, Deo G, Weckhuysen BM, Andreini A, Vuurman MA, de Boer M, Amiridis MD. *J. Catal.* 1996; **161**: 211.
- Ozkan US, Cai Y, Kumthekar M. *Appl. Catal. A* 1993; **96**: 365.
- Gasior M, Haber J, Machej T, Czeppe T. *J. Mol. Catal.* 1988; **43**: 359.
- Jehng J-M, Hu H, Gao X, Wachs IE. *Catal. Today* 1996; **28**: 335.
- Jehng J-M. *J. Phys. Chem. B* 1998; **102**: 5816.
- Bañares MA, Hu H, Wachs IE. *J. Catal.* 1995; **155**: 249.
- Bañares MA, Hu H, Wachs IE. *J. Catal.* 1994; **150**: 407.
- Hu H, Wachs IE. *J. Phys. Chem.* 1995; **99**: 10911.
- Oyama ST. *Chem. Intermed.* 1991; **15**: 165.
- Busca G, Elmi AS, Forzatti P. *J. Phys. Chem.* 1987; **91**: 5263.
- Busca G. *Catal. Today* 1996; **27**: 457.
- Chen K, Khodakov A, Yang J, Bell AT, Iglesia E. *J. Catal.* 1999; **186**: 325.
- Weckhuysen BM, Wachs IE. *J. Phys. Chem.* 1996; **100**: 14437.
- Bañares MA, Cardoso JH, Agulló-Rueda F, Correa-Bueno JM, Fierro JLG. *Catal. Lett.* 2000; **64**: 191.
- Das N, Eckert H, Hu H, Wachs IE, Waltzer JK, Feher FJ. *J. Phys. Chem.* 1993; **97**: 8240.
- Xie S, Iglesia E, Bell AT. *Langmuir* 2000; **16**: 7162.
- Damyanova S, Gómez LM, Bañares MA, Fierro JLG. *Chem. Mater.* 2000; **12**: 501.
- Pieck CL, Bañares MA, Vicente MA, Fierro JLG. *Chem. Mater.* 2001; **13**: 1174.
- Kasprzak MS, Leroi GE, Grouch SR. *Appl. Spectrosc.* 1982; **36**: 285.
- Carrier X, Lambert JF, Che M. *J. Am. Chem. Soc.* 1997; **119**: 10137.

76. Le Bihan L, Blanchard P, Fournier M, Grimblot J, Payen E. *J. Chem. Soc., Faraday Trans.* 1998; **94**: 937.
77. Stencil JM, Deihl JR, D'Este JR, Makovsky LE, Rodrigo L, Marcinkowska K, Adnot A, Roberge PC, Kaliaguine S. *J. Phys. Chem.* 1986; **90**: 4739.
78. Rocchiccioli-Delfcheff C, Amirouche M, Che M, Tatibouët JM, Fournier M. *J. Catal.* 1990; **125**: 2892.
79. Marcinkowska K, Adnot A, Roberge PC, Kaliaguine S. *J. Phys. Chem.* 1986; **90**: 4773.
80. Greenwood NN, Earnshaw A. *Chemistry of the Elements*. Pergamon Press: Elmsford, NY, 1989.
81. Tatibouët JM, Che M, Amirouche M, Fournier M, Rocchiccioli-Delfcheff C. *J. Chem. Soc., Chem. Commun.* 1988; 1260.
82. de Boer M, van Dillen AJ, Konigsberger DC, Geus JW, Vuurman MA, Wachs IE. *Catal. Lett.* 1991; **11**: 227.
83. Ramani NC, Sullivan DL, Ekerdt JG, Jehng J-M, Wachs IE. *J. Catal.* 1998; **176**: 143.
84. Dunn JP, Koppula PR, Stenger HG, Wachs IE. *Appl. Catal. B: Environ.* 1998; **19**: 103.
85. Briand LE, Hirt AM, Wachs IE. *J. Catal.* 2001; **202**: 268.
86. Burcham LJ, Briand LE, Wachs IE. *Langmuir* 2001; **17**: 6164, 6175.